An-Najah National University

Faculty of Graduate Studies

High-Pressure Band Structure and Structural Stability of EuTe and EuO Compounds

By

Rowaida Fakhri Mohammad Dewaikat

Supervisors

Dr. Mohammad S. Abu-Jafar

Co- Supervisor

Dr. Abdel-Rahman M. Abu-Labdeh

This Thesis is Submitted in Partial Fulfillment of the Requirements for the Degree of Master of Science in Physics, Faculty of Graduate Studies, An-Najah National University, Palestine.

2012

High pressure Band Structure and Structural Stability of EuTe and EuO Compounds

By

Rowaida Fakhri Mohammad Dewaikat

This Thesis was defended successfully on 24/5/2012 and approved by:

Defense Committee Members		**Signature**
Dr. Mohammad S. AbuJafar	**(Supervisor)**	**……**
Dr. Abdel-Rahman M. Abu-Labdeh	**(Co-Supervisor)**	**……**
Dr. Khawla Qamhieh	**(External Examiner)**	**……..…..**
Dr. Khaled Ilaiwi	**(Internal Examiner)**	**……..**

Dedication

I dedicate this work to the dearest people to my heart:

To my father

To my mother

To my husband

To my daughter Maysam

Acknowledgment

I do thank Allah for allowing me to finish this thesis successfully. My deepest gratitude and appreciation to my dear supervisors, Dr. Mohammed Abu-Jafar and Dr. Abdel-Rahman Abu-Labdeh for helping and guiding me with their deep knowledge in my field and for being patient with me to complete this thesis.

Thanks to the Defense Committee Members and also to all my family members: My father, my mother, my husband's family, brothers and sisters, especially for my husband for his encouragement, support and patient.

اقرار

أنا الموقع أدناه مقدم الرسالة التي تحمل العنوان:

High pressure Band Structure and Structural Stability of EuTe and EuO Compounds

أقر بأن ما اشتملت عليه هذه الرسالة إنما هو نتاج جهدي الخاص، باستثناء ما تمت الإشارة إليه حيثما ورد، وإن هذه الرسالة ككل أو أي جزء منها لم يقدم من قبل لنيل أة درجة أو لقب علمي أو بحث لدى مؤسسة تعليمية أو بحثية أخرى.

Declaration

The work provided in this thesis, unless otherwise referenced, is the researcher's own work, and has not been submitted elsewhere for any other degree or qualification.

اسم الطالبة: Student's name:

التوقيع: Signature:

التاريخ: Date:

Table of Contents

List of Tables

List of Figures

High-Pressure Band Structure and Structural Stability of EuTe and EuO Compounds

By
Rowaida Fakhri Mohammad Dewaikat
Supervisors
Dr. Mohammad S. Abu-Jafar
Dr. Abdel-Rahman M. Abu-Labdeh

Abstract

A First-Principles method is used to calculate the electronic, structural, and magnetic properties of the semiconductors EuTe and EuO in the rocksalt (RS), cesium chloride (CsCl) and zincblende (ZB) structures, using a self-consistent full-potential linearized augmented plane-wave (FP-LAPW) method within the local-spin-density functional approximation (LSDA) and the generalized gradient approximation (GGA). The program used in our calculation is WIEN2K-2010 code.

The effect of pressure on the electronic properties of (EuTe and EuO) was investigated, both compounds showed that the stable structure under normal pressure is rocksalt. Transition under high pressure was estimated for both EuTe and EuO compound from RS structure to CsCl structure, this transition is found to be about 12 GPa, 8 GPa, 10 GPa and 11 GPa for EuTe compound using PBE-GGA, LSDA, WC-GGA and PBEsol-GGA methods respectively, and the transition completed to CsCl structure for EuO compound at about 69 GPa, 61 GPa, 64 GPa and 63 GPa using PBE-GGA, LSDA, WC-GGA and PBEsol-GGA methods respectively.

It is found also that these compounds are semiconductors under normal or high pressure conditions in the three structures involved in this study. The

band structure calculations showed that EuTe compound has indirect band gap energy in RS and ZB structures, and direct but smaller band gap in CsCl structure. Also EuO band gap energy is indirect in RS and ZB structures but direct in CsCl structure.

In addition the comparison between different methods of calculation showed that the PBE-GGA method is better in predicting the lattice constant in the RS structure, but PBEsol-GGA and WC-GGA methods better in predicting the bulk modulus (B_o) and transition pressures (P_t).

CHAPTER 1

INTRODUCTION

Solid state physics is a fruitful study field, so that is not strange news that Noble prize committee decided in 2000 and 2007 to give it for scientists, such as *Zeros I. Alferov, Jack S. Kilby, and Herbert Kroemer* in 2000 and *Albert Fert, Peter Grünberg* in 2007[1], who worked until they got new ideas about using semiconductors in memories, spintronics, spin filtering devices and processors.

Currently, semiconductors are used in all communication fields as well as in all fiberglass communication fields. Out of these semiconductors are rare earth compounds. Rare earth elements (RE) presented by lanthanides and actinides are famous for their electrical and magnetic properties. These elements have large angular momentum and large centrifugal potential due to their large number of electrons. So, the electronic configuration for such elements ends with f orbital, which means that they have spin-orbit coupling [2].

Recently, lanthanides have cached new attention for its applications in technology due to their properties. Among these rare earth elements is Europium (Eu). As one member of RE family, Eu element has electronic configuration ends with $4f^{7}$. Thus, it has 7 unpaired electrons which are responsible for its magnetic properties. In addition, Eu is a ductile metal crystallizes in body centered cubic lattice [3]. It may found in divalent

(Eu+2) or trivalent (Eu+3) state. These two states are usually exist, but the divalent state is more stable because of its half filled *f* shell. Since the electronic configuration of Eu ends with $4f^7\ 6s^2$ [4], this element has the second lowest melting point and the lowest density of all lanthanides [3]. Besides, Eu is the most reactive element in all RE elements. Its reaction with air and water is fast like the reaction of calcium with water [5]. So, it is not expected to find it pure in nature, but instead it is found as compounds such as oxides. Out of these compounds are ferromagnetic semiconductors (FMS) [2], also named europium monochalcogenides formed from the reaction of Eu with an element from group VIA (i.e., O, S, Se or Te). The europium monochalcogenides are represented by EuX, where X is O, S, Se or Te. Because of their large magnetic moment, EuX show fully spin-polarized bands and colossal magnetoresistance (CMR) or giant magnetoresistance (GMR) [6]. In addition, EuX compounds have wide band gap energy. All of these properties make these compounds suitable for spintronics, memories and spin filtering devices. Moreover, these compounds are famous because of their magnetic and electric properties which make them fantastic tools for technological applications as well as fertile areas of academic research [2, 7-11].

One important compound among of EuX compounds is the EuO. Heathman *et al* [12] studied this compound experimentally using the dispersive X-ray diffraction technique and synchtroron radiation. They found that this compound crystallizes at normal conditions in the rocksalt (RS) structure ,

they also showed that EuO compound undergoes phase transition from RS phase to CsCl phase beginning at 47 GPa and the almost complete high pressure CsCl phase is at 63 GPa. They also found that the lattice constant (a_0) to be 5.145 Å. On the other hand, using Birch's equation, they found that the bulk modulus (B_0) and pressure first derivative (B') to be 114 GPa and 2.8, respectively. Using Murnaghan's equation, however, they found that the values of B_0 and B' are 118 GPa and 2.2, respectively [12]. In addition, Jayaraman *et al* [11] studied EuO using high pressure X-ray diffraction technique. They found that this compound undergoes NaCl to CsCl type transition at about 40 GPa. Also, they showed that a_0 equals to 5.14 Å and B_0 equals to 110±5 GPa in *RS* type. On the other hand, Moodera *et al* [13] examined EuO compound using the tunneling spin filter effect in tunnel junction, they found that the band gap energy is 1.12 eV for spin up polarized electrons.

Theoretically, this compound was examined using various methods, Wan *et al* [14] who used the full potential linearized–muffin-tin-orbital (FP-LMTO) method within the local spin density approximation (LSDA) with atomic Hubbard1for the self –energy to approximate the localized nature of Eu *f*-electrons. They pointed out that this compound is subjected to a change in its state under the influence of high pressure (~ 48 GPa) from RS phase to CsCl phase. Other lattice parameters such as B_0 and B' were found to be 105 GPa and 3.2, respectively. Gour *et al* [15] examined this system using the three-body interaction potential (TBIP) approach under high

pressure. They also emphasized that transition from NaCl to CsCl takes place at about 36 GPa with volume collapse of 7.7%.

Using the SIC-LSD method, Horne *et al* [16] found that the energy band gap of EuO is about 2.5 eV for spin up and 3.4 eV for spin down.

EuTe has also been examined theoretically and experimentally. Jayaraman *et al* investigated EuTe under high pressure experimentally using high pressure X-ray technique [10]. They found that transition from *RS* to CsCl type takes place at about 11.0 GPa, with lattice constant a_0= 6.591Å and bulk modulus of 40±5 GPa in the *RS* type. In addition, they have found that the lattice constant at transition point in NaCl phase is 6.22 Å, and in CsCl phase is 3.739 Å. Moreover, Kaminski *et al* [7] studied the properties of this compound under high pressure experimentally using X-ray magnetic circular dichroism (XMCD). They found that a_0 for EuTe in *RS* phase equals 6.598 Å [7].

Other researchers studied the magnetic properties of the EuTe compound such as Goncharenko and Mirebeau [17]. They pointed out that the structural phase transition occurs under high pressure from *RS* to CsCl phase. They also confirmed that transition occurs from anti-ferromagnetic (AFM) to ferromagnetic (FM) under pressure of 11.8 GPa and temperature of 10.9 K.

On the other hand, some theoretical calculations have been done for this compound. Singh *et al* [18] investigated this compound using tight binding

(TB) method, linear muffin-tin orbital (LMTO) method and atomic sphere approximation (ASA) within local density approximation (LDA). They showed that transition takes place at pressure of 9.89 GPa from *RS* to CsCl, with lattice parameter a_0=6.405Å and bulk modulus equals to 42.1 GPa and 101.7 GPa for *RS* and CsCl phases, respectively. At the transition point, the lattice parameter is reported to change from 6.405Å to 6.06Å in *RS* phase and 3.71Å in CsCl phase after transition [18]. Wan *et al* [14] studied EuTe using the LMTO method within the LSDA with atomic Hubbard1for the self-energy to approximate the localized nature of Eu *f* electrons. They showed that B_0 = 43 GPa, B'= 2.8 and the transition pressure (P_t=14 GPa). In addition, Horne *et al* [16] studied the energy band gap of EuTe. They got 0.4 eV for spin up and 1.1 eV for spin down.

The aim of this work, therefore, is to overcome the differences between the theoretical results and experimental results as mentioned before. In addition, this work is aimed to get better information about the accuracy of the methods Perdew-Burke Ernzerhof 96 (PBE-GGA), LSDA, Wu-Cohen 06 (WC-GGA) and Perdew *et al* 08 (PBEsol-GGA) that we use in this program. In this thesis, the numerical investigations based on first-principle study of ground state properties of EuTe and EuO compounds are done to investigate the stable electronic and magnetic structures under high pressure.

This thesis is divided into five chapters. Chapter 2 describes the concepts of the Density functional theory (DFT). Chapter 3 discusses the methods of

calculation as well as the computational details used in this work. Chapter 4 presents and discusses the structural, electronic and magnetic properties that we have obtained for EuTe and EuO compounds. In addition, this chapter summarizes a general conclusion for each compound of interest.

CHAPTER 2

DENSITY FUNCTIONAL THEORY

Introduction

Crystals are composed of particles (electrons) that move inside crystal beside positively heavy particles (nuclei) [19]. These systems or crystals are composed of inhomogeneous gas, which means lots of problems facing us in order to solve these systems. Therefore, solving equation of state of such systems is too complicated. So in this chapter, we are summarizing the steps which are taken in order to solve crystal ground state wave function and density of electrons.

2.1 The basic concepts of Density Functional Theory

In solid systems, one needs to get the electronic properties in order to control their applications. To study the ground state of such systems, we need to find the ground state wave function and density of state.

The crystal contains electrons and nuclei both are moving inside the crystal, but nuclei are much slower than electrons. The Schrödinger equation which describe any solid system is given by

$$\hat{H}\Psi = E\Psi, \qquad 2.1$$

where Ψ is the wave function, $\hat{H}$ is the Hamiltonian operator and E is energy eigen value. If we have N atoms so we have N nuclei and Z electrons. This means that we have many body problems of the order of N

+NZ [19]. In addition, these particles are interacting magnetically, so that this gives a quantum many body problem. Hence, the Hamiltonian for such system is given by

$$\hat{H} = \frac{-\hbar^2}{2}\sum_{I=1}^{N}\frac{1}{M_I}\nabla_I^2 - \frac{-\hbar^2}{2m}\sum_{i=1}^{n}\nabla_i^2 - \frac{1}{4\pi\epsilon_0}\sum_{I=1}^{N}\sum_{i=1}^{n}\frac{Ze^2}{r_{i,I}} + \frac{1}{8\pi\epsilon_0}\sum_{I=1}^{N}\sum_{J=1}^{N'}\frac{Z_I Z_J e^2}{r_{I,J}} + \frac{1}{8\pi\epsilon_0}\sum_{i=1}^{n}\sum_{j=1}^{n'}\frac{e^2}{r_{i,j}} \qquad 2.2$$

where M_I is the mass of nucleus at r_I, m is the mass of electron at r_i and Z_I, Z_J are the number of protons for I and J ions respectively. In equation (2.2), the first and the second terms are kinetic energy operators for the nuclei and electrons respectively, the third term is the electron-nuclear attraction, the fourth term is the nuclear-nuclear repulsion and the last term is the electron-electron repulsion [19]. It is very difficult to solve this equation analytically. So, many approximations are required to get nearly reasonable solutions.

2.2 The Born-Oppenheimer approximation

If we could get the properties of any system, then we can control its applications. Many methods of approximation were done to get the properties of solid systems precisely. Out of them is the Born-Oppenhiemer approximation. In this approximation, the electronic coordination is separated from the nuclear one. This means that the electrons are subjected to a constant potential from the nuclei, and the wave function of the system is separated into two functions: one for nuclear coordinates and the other

for electronic coordination. This implies that the nuclei are kept in static or adiabatic state with respect to electrons. Based on this assumption, the Hamiltonian can be written as [19]

$$\hat{H} = \frac{-\hbar^2}{2m}\sum_{i=1}^{n}\nabla_i^2 - \frac{1}{4\pi\epsilon_0}\sum_{I=1}^{N}\sum_{i=1}^{n}\frac{Ze^2}{r_{i,I}} + \frac{1}{8\pi\epsilon_0}\sum_{I,J=1}^{N}\frac{Z_I Z_J e^2}{r_{I,J}} + \frac{1}{8\pi\epsilon_0}\sum_{i,j=1}^{n}\frac{e^2}{r_{i,j}} \quad 2.3$$

where the kinetic energy vanishes for nuclei. In order to simplify equation (2.3), the Density Functional Theory (DFT) method is used. This method is depending on Thomas-Fermi model, with the theorems of Hohenberg-Kohn.

2.3 The Hohenberg-Kohn theorems

The Born-Oppenhiemer approximation reduced the problem to NZ order with electrons subjected under external potential, but still not enough to solve such system. Hohenberg and Kohn set two theorems to solve it [20]. These theorems are:

Theorem 1:

The external potential υ_{ext}(r), and hence the total energy, is a unique functional of the electron density n(r).

Theorem 2:

The ground state energy can be obtained variationaly. In other words, the density that minimizes the total energy is the exact ground state density.

The energy functional $E[n(r)]$, defined as the total energy as function of electrons density, introduced by Hohenberg-Kohn theorem can be written in terms of the external potential $\upsilon_{ext}(r)$ as follows

$$E[n(r)] = \int n(r)\, \upsilon_{ext}(r)\, dr + F[n(r)], \qquad 2.4$$

where $F[n(r)]$ is a universal function which depends only on the electron density n(r) .

In this model Ψ, which is used in the evaluation of the expectation value, must be the minimum, so that it gives the ground state energy. Thus, for non-degenerate state [19]

$$\mathrm{E[n(r)]} = \langle \Psi | \hat{H} | \Psi \rangle \qquad 2.5$$

This implies that the Hamiltonian should be given by

$$\hat{H} = \hat{F} + \hat{V}_{ext}, \qquad 2.6$$

where $\hat{F}$ is the electronic Hamiltonian, which is given by

$$\hat{F} = \hat{T} + \hat{V}_{ee}\,, \qquad 2.7$$

where $\hat{T}$ is the kinetic energy operator and $\hat{V}_{ee}$ is interaction operator. Therefore, $\hat{F}$ operator is the same for all N- electron system, and hence $\hat{H}$ is completely defined by the number of electrons (N), and the external potential ($\upsilon_{ext}(r)$).

This theorem can be proved by assuming that we have two different external potentials $\upsilon_{1ext}(r)$ and $\upsilon_{2ext}(r)$, both gives the same density $n_0(r)$.

The corresponding Hamiltonians $\hat{H}_1$ and $\hat{H}_2$ generated from the external potentials, will lead to different ground state wave functions, Ψ_1 and Ψ_2, but both Hamiltonians will give the same density $n_0(r)$. Because they are generated from potentials giving the same eigen values [19, 21].

2.4 The Kohn-Sham Formulation

Although Hohenberg-Kohn theorems are powerful, they couldn't offer a proper method to compute the ground state density. Kohn-Sham [22] devised a simple way to carry out DFT calculations.

They focused on mapping the interacting system with real potential, to fictitious non-interacting system, where the electrons are moving in effective "Kohn-Sham" single particle potential, $\upsilon_{eff}(r)$ or $\upsilon_{KS}(r)$. This method is still exact since it gives the same ground state density as the real system because they assume the non-interacting electrons have the same density of the real electrons [22, 23].

In this approximation the functional F [n(r)] is divided into three terms: the first two are known and represented most of the energy, the third term is a small unknown quantity. $F[n(r)]$ is given by:

$$F[n(r)] = T_s[n(r)] + E_H[n(r)] + E_{xc}[n(r)] \qquad 2.8$$

where $T_s[n(r)]$ is the kinetic energy of non-interacting electron gas of density $n(r)$, $E_H[n(r)]$ is the classical Hartree energy of the electrons given by

$$E_H[n(r)] = \frac{1}{2} \iint \frac{n(r)n(r')}{|r-r'|} dr\, dr' \quad 2.9$$

and $E_{xc}[n(r)]$ is the exchange-correlation energy. Now the Kohn-Sham potential $v_{eff}(r)$ is given by [24]

$$v_{eff}(r) = v_{ext}(r) + v_H(r) + v_{xc}(r), \quad 2.10$$

where $v_{xc}(r)$ is the exchange correlation potential defined as

$$v_{xc}(r) = \frac{\delta E_{xc}[n(r)]}{\delta n(r)} \quad 2.11$$

And $v_H(r)$ is the Hartree potential

$$v_H(r) = \frac{\delta E_H[n(r)]}{\delta n(r)} = \int \frac{n(r')}{|r-r'|} dr' \quad 2.12$$

We know that electrons are fermions which indicate that Kohn-Sham wave function is given by the determinant of single-particle orbital which leads to the lowest energy solution of the N one-electron Schrödinger equation:

$$\left[\frac{-\hbar^2}{2m} \nabla_i^2 + v_{eff}(r) \right] \varphi_i(r) = \varepsilon_i \varphi_i(r), \quad 2.13$$

This eigenvalue equation is particular representation of Kohn-Sham equations [22]. Here ε_i is the orbital energy of the corresponding Kohn-Sham's orbital function $\varphi_i(r)$, and the density of an N-electron system is

$$n(r) = \sum_i^N |\varphi_i(r)|^2 \quad 2.14$$

After solving the Schrödinger equation for this system, the density obtained is the same as the exact ground state density which is n(r) given by equation (2.14).

If n(r) is calculated then

$$\Psi_{GS} = \Psi\,[n(r)] \qquad 2.15$$

Or if we have Ψ_{GS} then we can get absolutely the *n(r)* of the ground state. This means that the wave function Ψ_{GS} is a unique function of the ground state density.

2.5 The Local – (Spin-) Density Approximation

The exchange correlation energy is represented by

$$E_{xc}[n(r)] = T[n(r)] - T_s[n(r)] + E_{ee}[n(r)] - E_h[n(r)], \qquad 2.16$$

where, $T_s[n(r)]$ and $E_{ee}[n(r)]$ are the exact kinetic and electron-electron interaction energies.

The E_{xc} term is not known and many approximations were done to describe this term depending on the electron density function.

The simplest approximation is the local density approximation (LDA). It is assumed that the exchange correlation energy at point (r) is equal to the exchange –correlation energy associated by a uniform electron gas that has the same density at the same point (r). Such a gas is completely

characterized by the density $n_\sigma(r)$, where $\sigma = \uparrow$ or $\downarrow$. The exchange-correlation energy per particle of that homogeneous gas is given by:

$$\varepsilon_{xc} = \varepsilon_x(n\uparrow, n\downarrow) + \varepsilon_c(n\uparrow, n\downarrow) \quad 2.17$$

ε_{xc} can be calculated, since the $\varepsilon_x(n\uparrow, n\downarrow)$ expression can be obtained by the Hartree Fock approximation [25], and the correlation energy $\varepsilon_c(n\uparrow, n\downarrow)$ is the analytic expression of Vosko Wilk and Nusiar (VWN) [26], which is based on *Monte Carlo* calculation of the ground state energy of homogeneous electron gas. So LDA and LSDA are dependent of the local density. Thus, the local energy is written by:

$$E_{xc}^{LDA}[n(r)] = \int \varepsilon_{xc} n(r) dr \quad 2.18$$

So the exchange correlation potential υ_{xc} can be presented as

$$\upsilon_{xc}(r) = \frac{\delta E_{xc}(r)}{\delta n(r)} = \frac{\partial n(r)\varepsilon_{xc} n(r)}{\partial n(r)}, \quad 2.19$$

where $\varepsilon_{xc} n(r) = \varepsilon_{xc}^{hom} n(r)$, and $\varepsilon_{xc}^{hom} n(r)$ is the exchange-correlation energy corresponding to a homogeneous electron gas of density *n(r)*. The most common formula used for $\varepsilon_{xc}^{hom} n(r)$ is that of Perdew and Zunger [27, 28], which is based on Quantum Monte Carlo calculations of the homogeneous electron gas generated by Ceperly and Alder [28, 29] to fix the interpolation formula.

Despite its simplicity this method worked good in solid systems and used well in solid state calculations, but it did not work well in chemistry due to the tendency of over binding which cause too small lattice constants.

2.6 The Generalized Gradient Approximation

The beginning for the generalized gradient approximation (GGA) was an extension to the LDA, where Hohenberg and Kohn proposed the extension for the LDA which known as the gradient expansion approximation (GEA) [20]. The GEA is a series expansion of increasingly higher order density gradient terms. It was tested for atoms and molecules but it was a complete failure.

The reason for (GEA) failure was because of the exchange potential term. Despite its failure, this method established the basics of GGA which now is popularly used in exchange correlation energy in condensed matter.

The problems faced GEA was overcome by Perdew and co-workers [30] by presenting an analytic function known as the enhancement factor, $F_{xc}[n(r), \nabla n(r)]$ which modified the LDA energy density to become:

$$E_{xc}^{GGA}[n(r)] = \int \varepsilon_{xc}^{hom}[n(r)]n(r)F_{xc}[n(r), \nabla n(r)]dr \qquad 2.20$$

The GGA resolved the problem and failure of GEA of the exchange potential. Also overcome the problem of the over binding of LDA which caused small lattice parameters.

2.7 The self consistent field in DFT

As mentioned early through Hohenberg –Kohn theorems, the ground state energy is that which minimizes energy. But when LDA approximation used this variation is no more applied on such problem. In order to get the

ground state in such condition, self consistent is needed. This means that the density must be refined iteratively by solving equations (2.13) and (2.14) alternately and the following flow chart is describing this method.

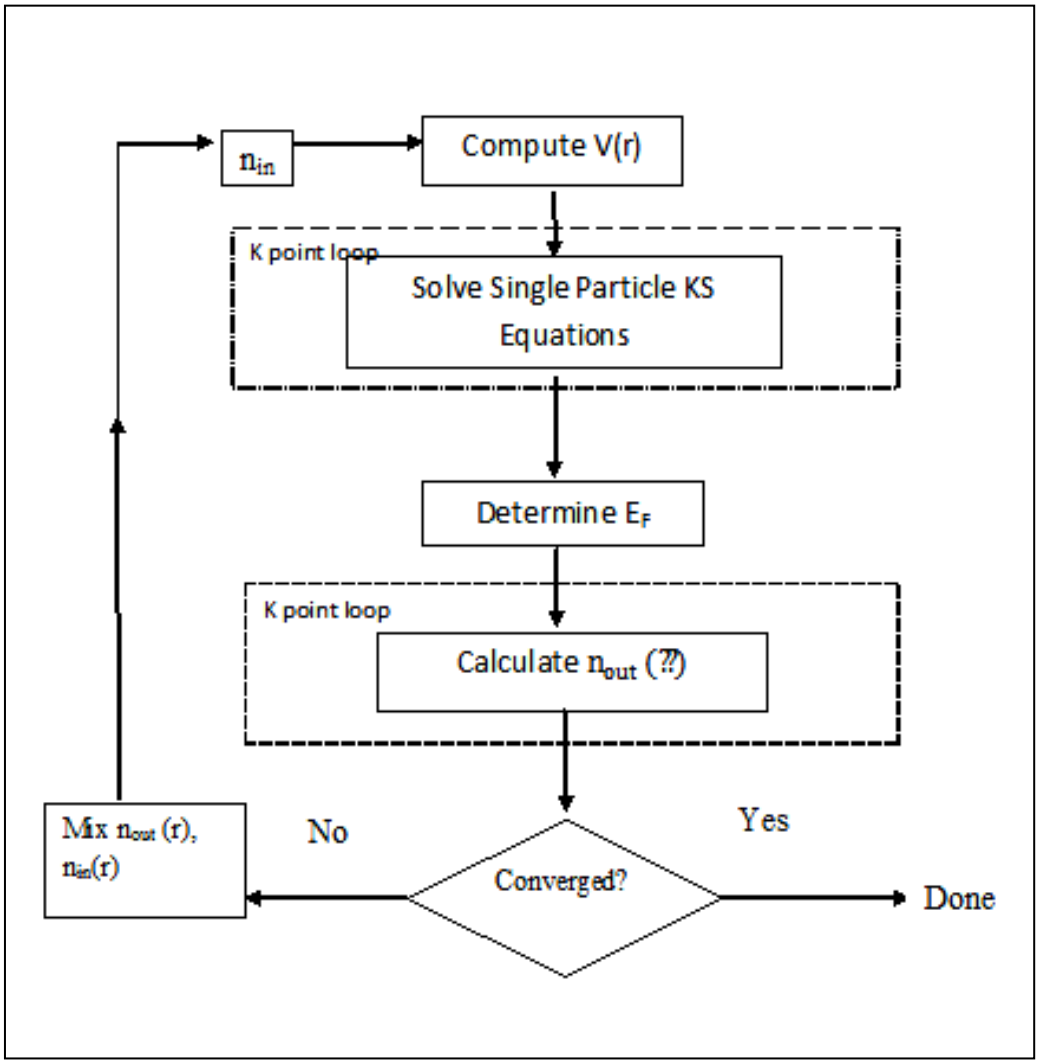

Figure 2.1: Flowchart for self consistent density functional calculations

The charge density is constructed from equation 2.14 and then mixed with the input to give a refined input for the next iteration. The simplest mixing is given by the following equation

$$n_{in}^{i+1} = (1-\alpha)n_{in}^{i} + \alpha n_{out}^{i}\,, \qquad 2.21$$

where the superscript refers to the iteration number and α is the mixing parameter. Other mixing procedures are followed to avoid the decreasing of the radius of convergence [31].

CHAPTER 3

METHOLOGY

3.1 Augmented plane wave method

The idea of this method was started in 1937 by Slater [32], when he used the so-called muffin-tin approximation to construct a set of basis functions. Therefore, this method is called augmented plane wave. The augmented plane wave method consists of plane waves, in regions of slowly varying potential, and atomic orbital like functions, in regions of faster varying wave functions.

3.2 Basis functions in muffin-tin potential

Although the potential in crystal varies continuously, the crystal space in the muffin-tin approximation is divided into two regions as shown in Figure 3.1. The first region is called the muffin-tin (MT), which contains non-overlapping spheres, while the other region is the rest of the crystal space, which is called the interstitial region. The division of the crystal, therefore, divides the potential into two parts. The first potential is nearly spherical symmetric potential, which is located in the MT region; while the second potential is a flat potential, which is located in the interstitial region.

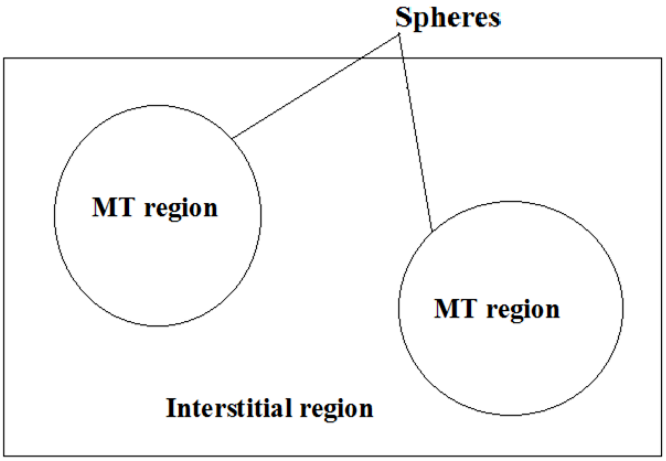

Figure 3.1: Adaption of the basis set by dividing the unit cell into atomic spheres and interstitial regions.

These basis are set due to the assumption that wave function and potential near to the nuclei are similar to those in atom, but in the interstitial region they are smoother [32].

According to this method, the wave function (φ) is given by

$$\varphi(\vec{r}) = \begin{cases} \sum_{lm} a_{lm}^{\alpha} u_{lm}^{\alpha}(r,\varepsilon) Y_{lm}(\vec{r}), & r < R_{\alpha} \\ \Omega^{1/2} \sum_{G} C_G \exp\left(i(\vec{k}+\vec{G}).\vec{r}\right), & r \in I \end{cases} \qquad 3.1$$

where Ω is the unit cell volume, $\vec{r}$ is the position inside sphere α, $\vec{k}$ is the wave vector in the irreducible Brillouin zone, Y_{lm} is the spherical harmonic function of angular momentum of quantum numbers *l* and *m* and u_{lm} is the numerical solution, which satisfies the radial Schrödinger equation

$$\left[-\frac{d^2}{dr^2} + \frac{l(l+1)}{r^2} + V(r) - E_l\right] r u_{lm}(r) = 0 \qquad 3.2$$

where *V* is the spherical component of the potential and for fixed energy E_l, u_l (r) must be defined at $r = 0$. To guarantee the continuity of the potential on the spheres boundaries, the constraint is done by defining the u_{lm} in terms of plane wave coefficients (C_G) as.

$$u_{lm} = \frac{4\pi^{l}}{\Omega^{1/2} u_l(R)} \sum_G C_G J_l(|k+g|)\, Y_{lm}^{*}\left(\vec{k}+\vec{G}\right) \qquad 3.3$$

Where C_G are the plane wave coefficients (the plane waves entitled by G means augmented plane waves).

3.3 Linearized Augmented Plane Wave

The problem of the previous approximation is that the wave function varies strongly with energy, which means that the wave function depends on energy in APW method. In order to get basis set energy independent, we introduce the linearized augmented plane wave (LAPW). This method is the most accurate method for performing electronic structure calculations of crystals with independent energy wave functions.

LAPW was developed by Andersen [33] in which the radial wave function is linearized by taking a linear combination of a solution *u* at fixed energy and its derivative u̇. So, the basis of LAPW is the same as in APW basis function with small difference in the muffin-tin region as shown below

$$\varphi(\vec{r}) = \begin{cases} \sum_{lm}[a_{lm}^{\alpha} u_{lm}^{\alpha}(r) + b_{lm}^{\alpha} \dot{u}(r)] Y_{lm}(\vec{r}), & r < R_{\alpha} \\ \Omega^{1/2} \sum_G C_G \exp\left(i\left(\vec{k}+\vec{G}\right).\vec{r}\right), & r \in I \end{cases} \qquad 3.4$$

where b_{lm} are coefficients of the energy derivative similar to that a_{lm}. So, the basis functions inside the spheres are linear combination of radial functions $u_l(r)Y_{lm}(r)$ and their derivatives $u_l(r)Y_{lm}(r)$ and $\dot{u}(r)Y_{lm}(\vec{r})$ which are the augmented functions. The $u_l(r)$ are defined in equation (3.3), while the $\dot{u}(r)$ are defined as

$$\left[-\frac{d^2}{dr^2} + \frac{l(l+1)}{r^2} + V(r) - E_l\right] r\dot{u}_{lm}(r) = r u_{lm}(r) \qquad 3.5$$

The LAPW basis yielding larger matrix and this gives slower convergence, but still LAPW is a great important development over the energy dependent, and in many practical calculations the matrix of LAPW is only diagonalized once.

The LAPW basis yielding larger matrix and this gives slower convergence, but still LAPW is great important development over the energy dependent, and in many practical calculations the matrix of LAPW is only diagonalized once. Since LAPWs are now more flexible to form plane waves inside spheres because they are now performed using two ($_{v}$). To continue this flexibility [34], the basis must have continuous derivatives and higher plane wave cut-offs to give a level of convergence. Another problem is that $u_{lm}(R)$ gives zero, which means that decoupling between plane waves and radial functions happened. To solve such problem, the Kohn-Sham equations are expanded using the linear variational method

$$\Psi_{\mathrm{k}} = \sum_n C_n \varphi_{kn}, \qquad 3.6$$

where C_n coefficients are determined by Rayliegh-Ritz variational principle, and the convergence of the basis is controlled by cut-off parameter $R_{mt}*K_{max}$, with R_{mt} is the smallest atomic sphere, K_{max} is the largest *Kn* vector in equation (3.6) [35].

3.4 The linearized augmented plane waves plus local orbitals

Some metals have high-lying core states (e.g. electrons in p-state which are not contained entirely in the muffin-tin), so that their energy is too high to

be neglected and cannot be described using the energy *E*. Therefore, many ways are taken to solve such problem. One of them is using local orbitals [36]. The way to do so is to define another orbital function. With u_l and $\dot{u}_l$ term, φ is given by

$$\varphi(\vec{r}) = \begin{cases} \left[a_{lm}^{\alpha,lo}\ u_{lm}^{\alpha,lo}(r) + \ b_{lm}^{\alpha,lo}\dot{u}(r)\right]Y_{lm}(\vec{r}), & r < R_\alpha \\ 0, \quad r\ \in I \end{cases} \qquad 3.7$$

The boundary conditions are the same as that LAPW basis, and it is evaluated at the same fixed energy as the corresponding APWs. The coefficients a_{lm} and b_{lm} are determined using normalization and are chosen such, that this local orbitals vanishes at the muffin-tin boundary.

There is an advantage of this method where it converges faster than the LAPW, because it includes few local orbitals [35, 37].

3.5 The Full Potential calculation (FP-LAPW)

In the solid systems, such as opened or layered systems, the muffin-tin approximation is no more useful due to disagreements with experimental results. Therefore, no shape approximation is better in such condition. The potential in no shape approximation is expanded as follows

$$\mathrm{V}(\vec{\mathrm{r}}) = \begin{cases} \sum_{\mathrm{lm}} \mathrm{V}_{\mathrm{lm}}\, \mathrm{Y}_{\mathrm{lm}}(\vec{\mathrm{r}}), \ \text{inside sphere} \\ \sum_{\mathrm{K}} \mathrm{V} \exp\left(\mathrm{i}\vec{\mathrm{K}}\vec{\mathrm{r}}\right), \ \text{out side sphere} \end{cases} \qquad 3.8$$

This general form is called full-potential calculation. In FP-LAPW method one can choose the radii of spheres without getting the appropriate choice.

In MT approximation, however, one must choose the spheres radii in the average of the real values [35].

3.6 Computational Details:

Our calculations are performed using the scalar relativistic full-potential linearized augmented plane wave (FP-LAPW) [35] approach based on the density functional theory with the LDA and GGA approximations [38]. We also used the Ceperly-Alder [29] forms for exchange-correlation energy as parameterized by Perdew and Wang [39]. In this work we used the most recently version of Vienna package WIEN2K_2010 code [37].

The atomic configuration of Eu, Te and O are [*Xe*] $4f^7\ 6s^2$, [*Kr*] $4d^{10}\ 5s^2\ 5p^4$ and [*He*] $2s^2\ 2p^4$, respectively. The valence electrons for Eu, Te and O are $6s^2\ 4f^7\ 5d^{10}$, $5s^2\ 5d^8\ 5p^6$ and $2s^2\ 2p^4$, respectively.

The core electrons are expanded in self consistency with spherical approximation. The muffin tin radius (R_{MT}) around each atom is chosen in each compound differently for the same atom. R_{MT} for Eu and Te in EuTe is chosen to be of 2.9 Å and 2.6 Å, respectively. While in EuO the R_{MT} is chosen to be 2.6 Å for Eu and 1.9 Å for O. Table 3.1 summarizes the input data for both compounds EuTe and EuO.

Table 3.1: The input parameters of both compounds in the WIEN2K-2010.

Input parameters	EuTe	EuO
l_{max}	10	10
$R_{MT}*K_{max}$	7.5	9.0
k- points	200	500
Reduced k points(k-mesh)	10	20

The integration over the Brillouin zone is performed using Monkhorst and Pack [40] mesh, reduced as shown in Table 3.1. The convergence of the total energy is taken to less than 0.1 mRyd.

The calculation of total energy is examined under high-pressure, in addition to the calculation of the lattice constant, the bulk modulus and the first derivative of the bulk modulus are done using Murnaghan's equation of state [41]

$$E(V) = E_o(V) + \frac{B_o V}{B'(B'-1)}\left[B_o\left(1-\frac{V_o}{V}\right) + \left(\frac{V_o}{V}\right)^{B'} - 1\right], \qquad 3.9$$

where E_o, V_o , B_o and B' are the energy, volume, bulk modulus and the pressure derivative of the bulk modulus, respectively, at equilibrium.

3.6.1 Rocksalt (RS) structure

In this structure, there are two atoms per unit cell positioned at (0, 0, 0) and (0.5, 0.5, 0.5). The following graph illustrates the scheme of the cubic rock salt structure.

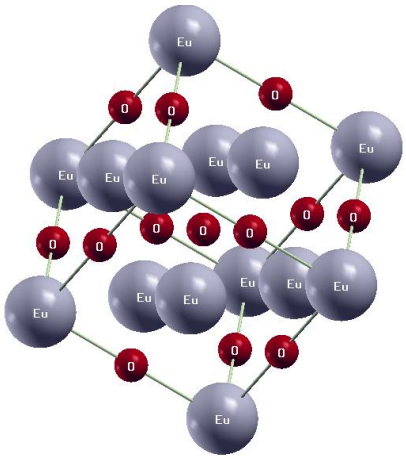

Figure 3.2: The schematic illustration of the cubic rocksalt structure.

3.6.2 Cesium Chloride (CsCl) structure

This structure like rocksalt has two atoms per unit cell, the positions of the first atom is at (0, 0, 0) and the position of the other atom is at (0.5, 0.5, 0.5) as shown in the schematic Figure 3.3

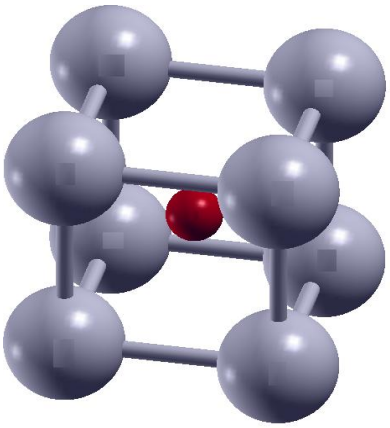

Figure 3.3: The schematic illustration of the cubic cesium chloride structure.

3.6.3 Zincblende (ZB) structure

The ZB structure consists of two atoms positioned at (0, 0, 0) and (0.25, 0.25, 0.25).

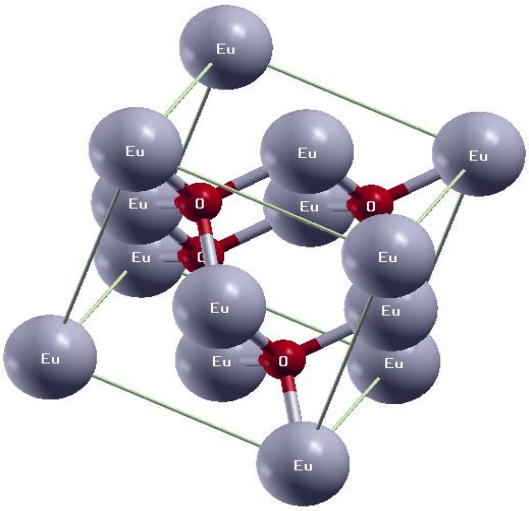

Figure 3.4: The schematic illustration of the cubic zincblende structure.

CHAPTER 4

RESULTS AND DISCUSSIONS

The results of the present work for both EuTe and EuO compounds using WIEN-2k code are displayed and discussed in this chapter. These results include magnetic states, band structures and the transition pressures.

4.1 Magnetic properties

4.1.1 Magnetic properties of EuTe compound

In order to obtain the ground state properties, optimization process is carried out in the magnetic and nonmagnetic states of the *RS* phase. In fact, the magnetic state calculations are performed using spin polarized for ferromagnetic. Rotation matrix is used to reverse the spin up and down for antiferromagnetic. On the other hand, nonmagnetic state calculations are carried out using non-spin polarized band structure.

In order to get the stable magnetic phase of EuTe we have studied the magnetism by involving the spins up and down of electrons. It is worth noting that the calculations are done in rocksalt (*RS*) phase.

Using the PBEsol-GGA method [38], figure 4.1 shows the variation of total energy with unit cell volume for both nonmagnetic and magnetic

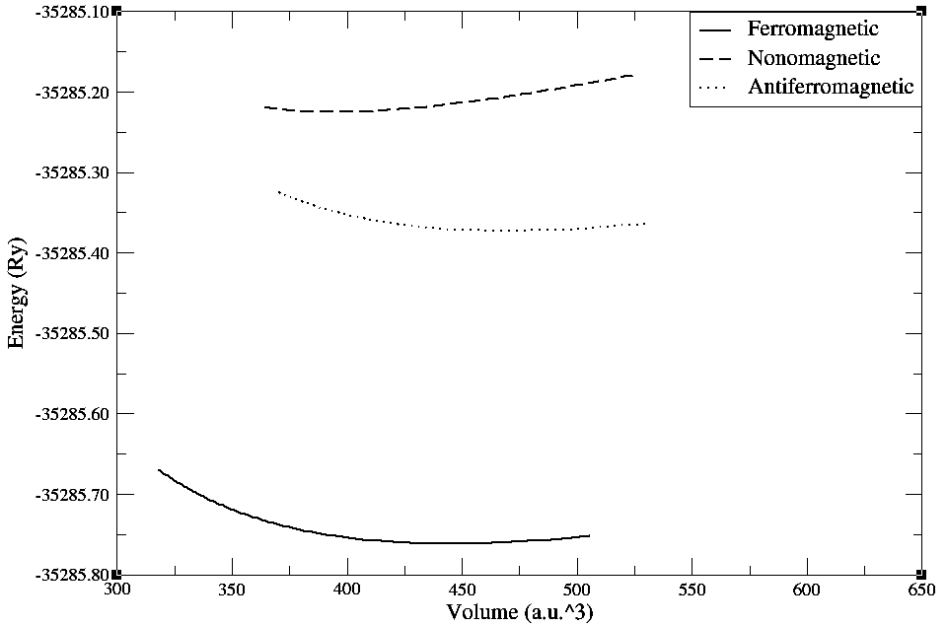

Figure 4.1: Calculated total energy with unit cell volume for non-magnetic, anti-ferromagnetic and ferromagnetic states of EuTe compound in the *RS* phase.

(ferromagnetic and antiferromagnetic) states of EuTe in the *RS* phase. Figure 4.1 clearly shows that the stable state of the EuTe compound is ferromagnetic state, since the total energy of this magnetic state is the minimum as presented in Table 4.1.

Table 4.1: The values of the total minimum energy of EuTe in RS structure using PBEsol-GGA method for magnetic and nonmagnetic states.

The state	**Nonmagnetic**	**Magnetic**	
		Ferromagnetic	**Antiferromagnetic**
Total energy (Ry)	-35285.2148	-35285.75104	-35285.3728

This implies that the ferromagnetic phase is the stable state. In addition, a transition from magnetic to nonmagnetic does not seem to happen. Because the stable magnetic state is the ferromagnetic, the rest of the calculations

are done for EuTe compound using the ferromagnetic state as ground state for the calculations in the three structures. These results are in good consistency with the other calculated results [18].

4.1.2 Magnetic properties of EuO compound

To get the stable magnetic state for EuO, Figure 4.2 shows the variation of total energy with the unit cell volume for both nonmagnetic and magnetic (ferromagnetic) states of EuO in the rocksalt phase.

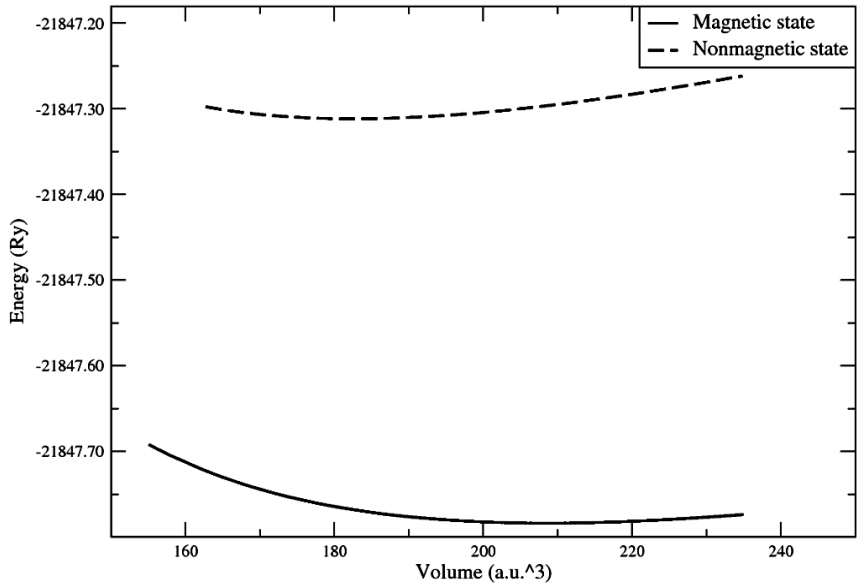

Figure 4.2: Calculated total energy with unit cell volume for both non-magnetic and magnetic states of EuO in the *RS* phase.

It is obviously shown from Figure 4.2 that the stable magnetic state of EuO is the one with the smallest energy, which is the ferromagnetic state. In

addition, Figure 4.2 shows that the transition from magnetic to nonmagnetic is not possible. The following table summarizes the total minimum energy of each state at unit cell volumes.

Table 4.2: The values of the total minimum energy of EuO in RS structure using PBEsol-GGA method for magnetic and nonmagnetic states.

The state	**Nonmagnetic**	**Magnetic (Ferromagnetic)**
Total energy (Ry)	-21847.311617	-21847.783654

Table 4.2 shows that the energy of the nonmagnetic state is larger than the energy of the magnetic state, this confirms that the magnetic state is the most stable one. Also, the rest of the calculations of EuO compound are done using ferromagnetic state.

4.2 Structural properties and structural phase transition:

4.2.1 Structural properties of EuTe compound:

The EuTe compound is studied in RS, CsCl and ZB structures. In RS and CsCl structures, as mentioned before, there are two atoms per unit cell. In RS and CsCl structures, Eu atom positioned at (0, 0, 0) and Te atom positioned at (0.5, 0.5, 0.5). While in ZB structure, Eu atom positioned at (0, 0, 0) and Te atom positioned at (0.25, 0.25, 0.25). Figure 4.3 illustrates

the scheme of the cubic rocksalt, cesium chloride and zincblende structures.

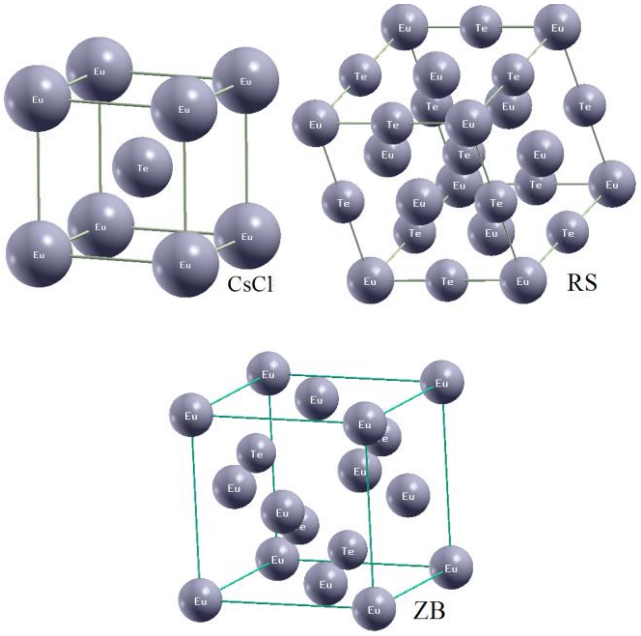

Figure 4.3 The schematic illustration of the cubic rocksalt, cesium chloride and zincblende structures.

calculation is needed for each structure. Figures 4.4, 4.5, 4.6 and 4.7 show the variation of total energy with unit cell volume using, PBE-GGA, LSDA W-Cohon and PBEsol-GGA approximations, respectively. The calculated energies are fitted by Murnaghan's equation of state (Equation 3.9) [41].

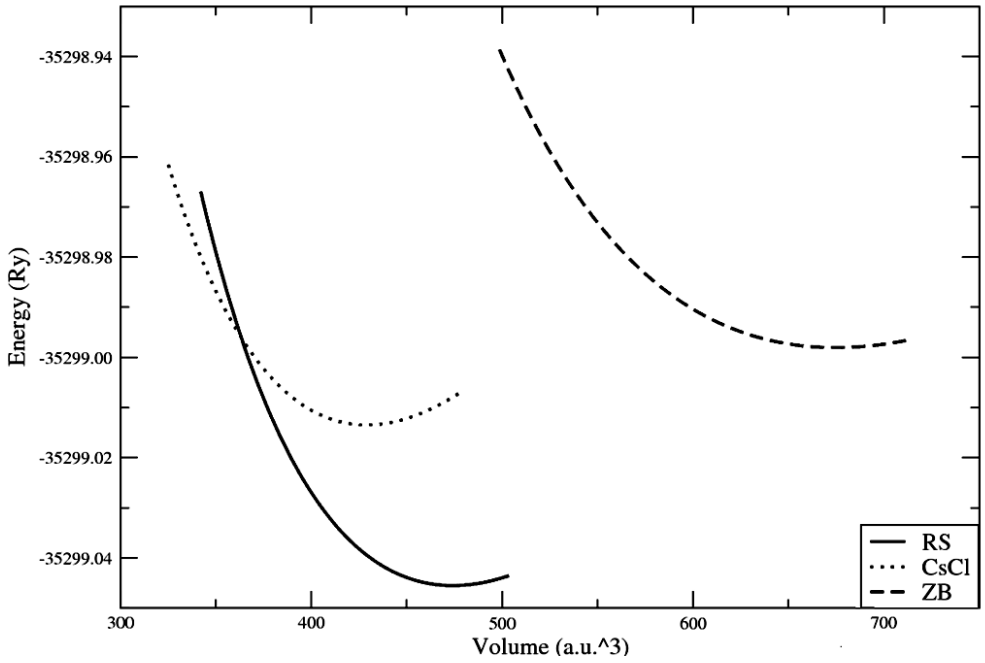

Figure 4.4: Total energy as function of volume of EuTe compound in RS, CsCl and ZB phases using PBE-GGA method.

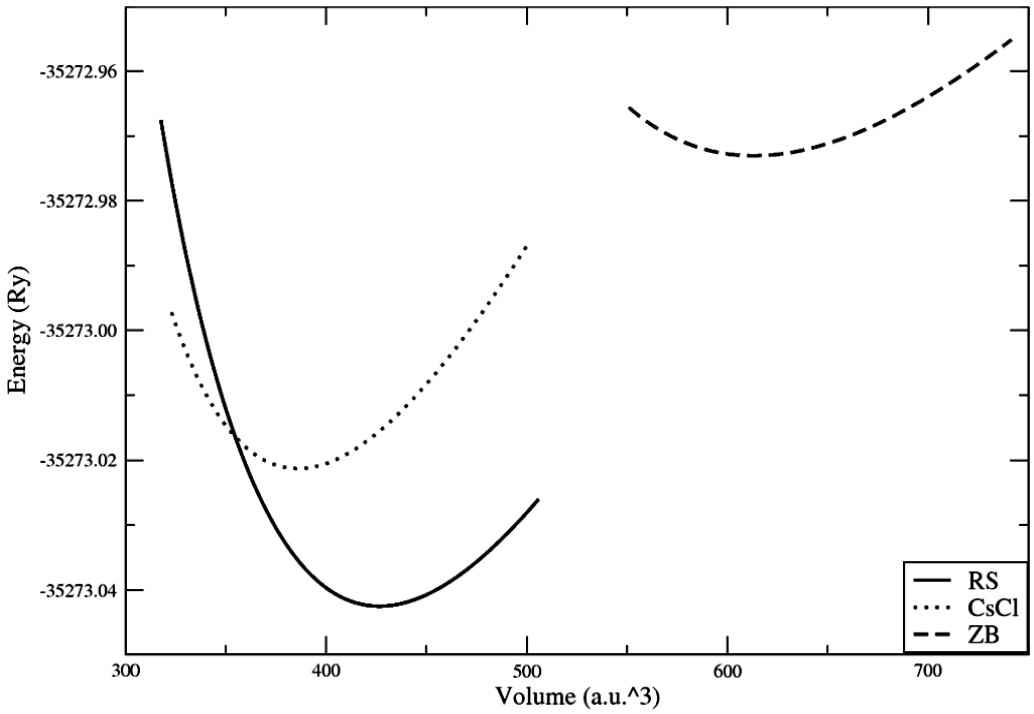

Figure 4.5: Total energy as function of volume of EuTe compound in RS, CsCl and ZB phases using LSDA method.

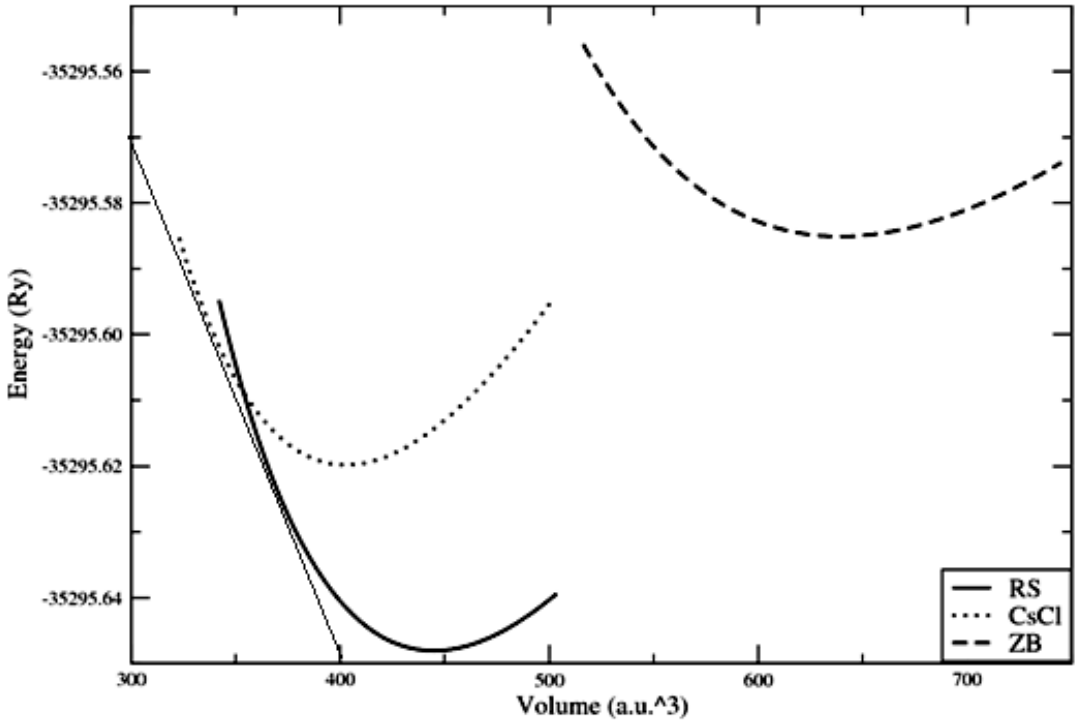

Figure 4.6: Total energy as function of volume of EuTe compound in RS, CsCl and ZB phases using WC-GGA method.

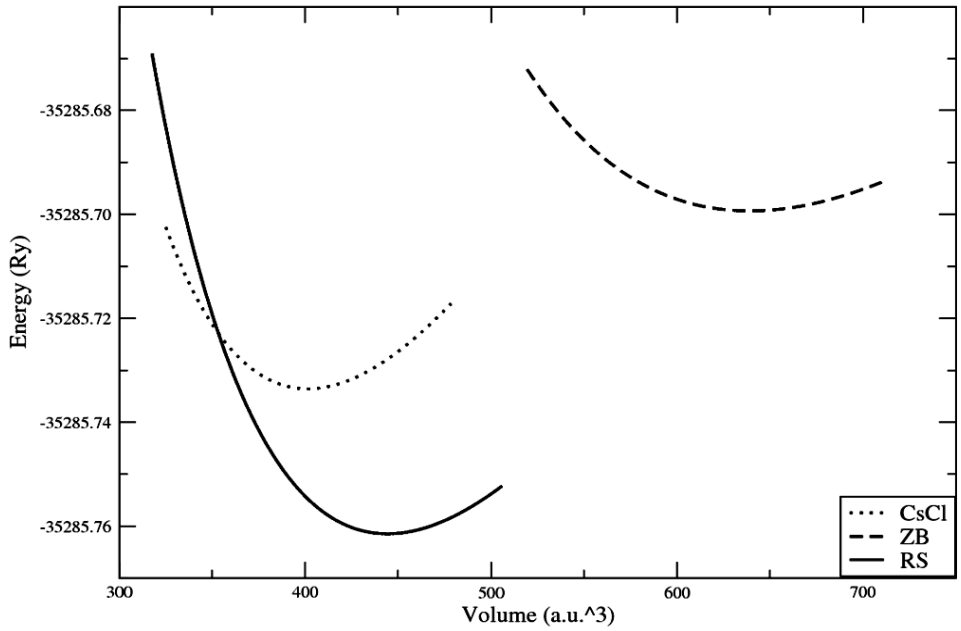

Figure 4.7: Total energy as function of volume of EuTe compound in RS, CsCl and ZB phases using PBESOL-GGA method.

Figures 4.4, 4.5, 4.6 and 4.7 show that the stable structure of EuTe is the RS structure, where the curves of both RS and CsCl structures intersects at the range of the minimum energy, but ZB structure has large minimum energy so it is not stable at any high pressure value. So, these figures pointed out that the transition from RS to ZB cannot occur, but transition from RS to CsCl can occur. This result is compatible with the experimental results very well [10, 13, 14, 18].

The present calculations of the lattice constant (a_o), bulk modulus (B_o) and the pressure derivative of the bulk modulus (B') as well as their available experimental and theoretical values are listed in Table 4.3. It is worth noting that the lattice constant a_o is evaluated using the relation of the unit cell volume at minimum energy (V_0) with a_o ($V_0 = a_o^3/4$ for the RS and ZB structures, while $V_0 = a_o^3$ for the CsCl structure).

Table 4.3: Lattice constants a_o, bulk modulus B_o and pressure derivative of the bulk modulus B' of EuTe compound in RS, CsCl and ZB structures using different methods of calculation.

Structures		Present work					Other calculations	Experimental results
		PBE-GGA	LSDA	WC-GGA	PBEsol-GGA	LDA		
RS	a_o (Å)	6.549	6.323	6.411	6.409	6.0937	6.405[a]	6.59[b], 6.598[c]
	B_o (GPa)	34.984	44.546	40.457	39.746	61.647	43[d], 42.1[a]	40 ± 5 [b]
	B'	4.079	4.502	4.422	4.34	5.6	2.8[d]	-
CsCl	a_o (Å)	3.99	3.852	3.907	3.903	3.712	3.71[a]	3.739 [b]
	B_o (GPa)	39.7	48.13	43.58	43.52	59.772	101.7 [a]	-
	B'	3.4	4.1	4.06	4.01	3.82	-	-
ZB	a_o (Å)	7.366	7.135	7.235	7.235	6.95	-	-
	B_o (GPa)	22.3023	27.949	24.513	24.713	32.9	-	-
	B'	4.028	4.894	4.307	4.14	5.1	-	-

[a] Ref. [18], [b] Ref. [10], [c] Ref. [7], [d] Ref. [14],

Table 4.3 shows that the lattice constant obtained using the PBE-GGA method (a_o = 6.549 Å) for EuTe in RS structure is close to the experimental value (6.591 Å) [10]. Moreover, the value of the bulk modulus obtained using the WC-GGA and PBEsol-GGA methods (40.5 and 39.7 GPa, respectively) are in excellent agreement with the experimental value (40 ± 5 GPa) [10].

Also, the results of the cesium chloride structure showed that the lattice constant is very close to the experimental results with no more than 3%

percentage error. On the other hand, we found a difference between our results and other theoretical results in the bulk modulus value (B_o). After studying the value of this variable, and retesting the compound in the cesium chloride in the same way that was done on the value 101.7 GP using LDA method [18], a difference was found in the values. We have discovered the error that occurred when the researchers calculated the value of the variable B_o and this is obviously clear in figure 4.8.

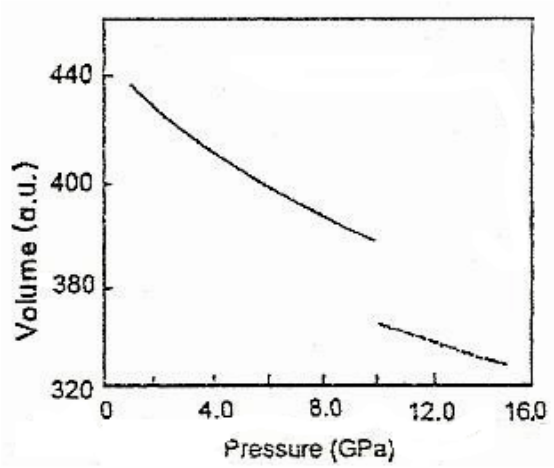

Figure 4.8: V-P curve in CsCl structure for EuTe compound [18].

Figure 4.8 shows that the scale of the y-axis in their article is not equal, and this resulted in an error in the calculation of the variable. Therefore, the value of B_o was calculated again using the slope of the tangent line from figure 4.8 using the following equation

$$B_o = -V_o \frac{\partial P}{\partial V} \qquad 4.1$$

The result was that the value of B_o ~ 60 GPa and not 101.7 GPa, and this corresponds well with our results that we have obtained, especially using the LDA method.

In addition the comparison with experimental results cannot be completed since there are no experimental results according to our knowledge.

4.2.2 Structural phase transition of EuTe compound:

This study concentrates on the phase transitions under high pressure. The transition pressure is evaluated using the relation of the derivative of total energy with respect to the volume of the unit cell.

$$P_t = -\frac{\Delta E}{\Delta V} \qquad 4.2$$

As introduced before, Figures 4.4, 4.5, 4.6 and 4.7 clearly show that the transition can occur from RS to CsCl.

In order to calculate the transition pressure a common tangent line is drawn to intersect with both curves of RS and CsCl structure as shown in figure 4.6, then using equation 4.2 we get the values of the transition pressure which are listed in Table 4.4.

Table 4.4: The transition pressure for EuTe from RS to CsCl using different methods of calculation.

Method	Transition Pressure (P_t) in GPa		
	Present work	**Other calculations**	**Experimental results**
PBE-GGA	12.56	-	11[c]
LSDA	8.117	9.89[a], 14[b]	
WC-GGA	10.437	-	
PBEsol-GGA	11.14	-	

[a] Ref. [18], [b] Ref. [14], [c] Ref. [10].

Table 4.4 shows that the present results of transition pressure ranges from 10-12 GPa using PBE-GGA, WC-GGA and PBEsol-GGA methods, which are in good agreement with the experimental results as well as with other calculations using different methods. Table 4.4 also indicates that the value of the transition pressure using the LSDA method is under estimated.

Furthermore, the calculated volume just before the transition (in rocksalt structure) is 379.1 a.u.^{3}, where it is 349.9 a.u.^{3} just after transition (in CsCl structure). The variation of the lattice parameter a_0, at the transition point is estimated to be from 6.54 Å to 6.076 Å in *RS* phase, which corresponds to the experimental values from 6.591 Å to 6.222 Å [10]. The results are comparatively agree well with the experimental results and with other theoretical calculations. The experimental results done by Jayaraman *et al* [10] give a variation in the lattice parameter a_o from 6.591 to 6.222 Å.

Theoretically, Singh *et al* [18] found that a_o changes from 6.405Å to 6.06Å.

4.2.3 Structural properties of EuO compound

The Europium Oxide is also studied in the RS, CsCl and ZB structures. These structures, as mentioned before, contain two atoms per unit cell as shown in Figure 4.9.

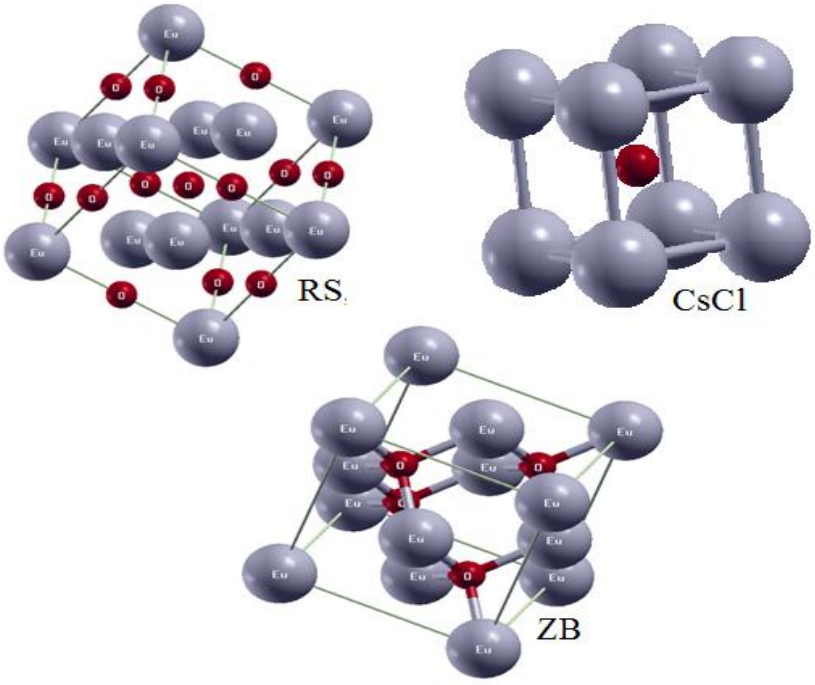

Figure 4.9: The schematic illustration of the cubic rocksalt, cesium chloride and zincblende phases of EuO compound.

Figures 4.10, 4.11, 4.12 and 4.13 show the total energy versus volume of the EuO compound in the RS, CsCl and ZB structures using PBE-GGA, LSDA, WC-GGA and PBEsol-GGA methods, respectively.

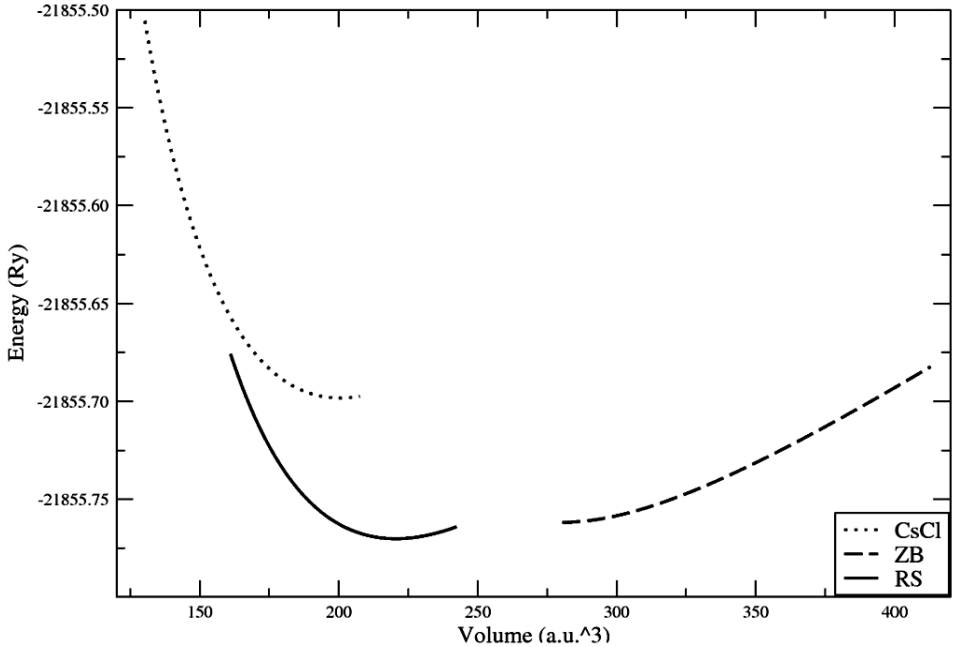

Figure 4.10: Total energy as function of volume of EuO compound in RS, CsCl and ZB phases using PBE-GGA method.

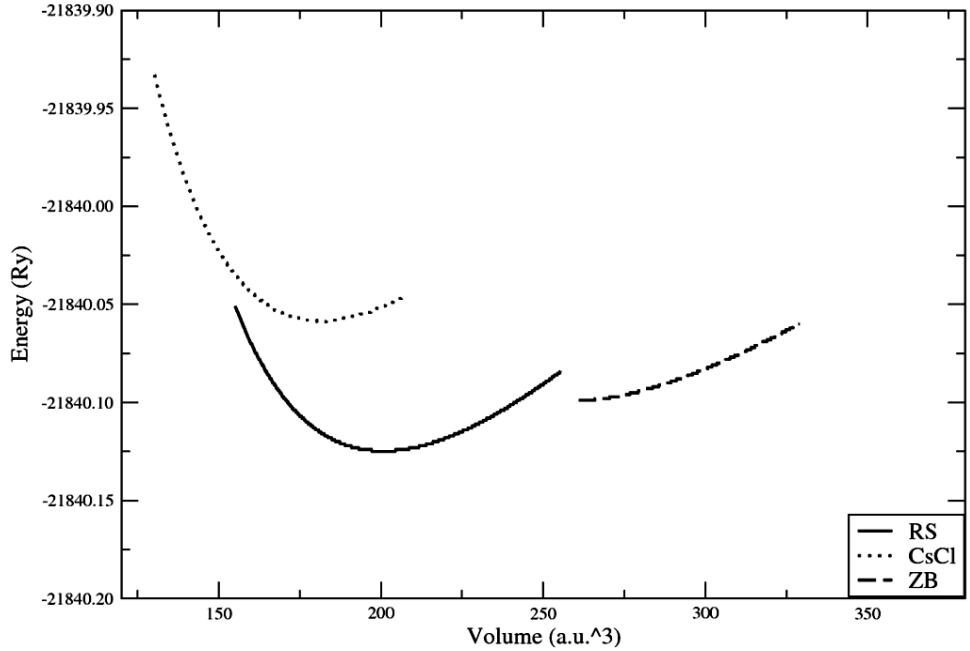

Figure 4.11: Total energy as function of volume of EuO compound in RS, CsCl and ZB phases using LSDA method.

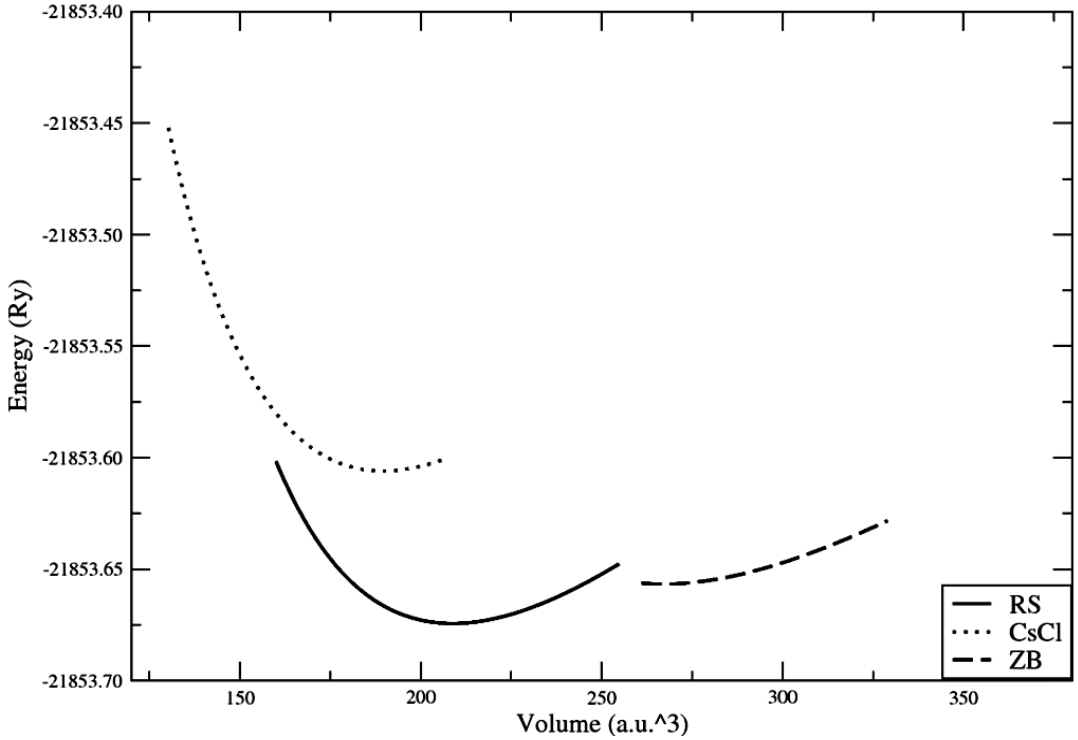

Figure 4.12: Total energy as function of volume of EuO compound in RS, CsCl and ZB phases using WC-GGA method.

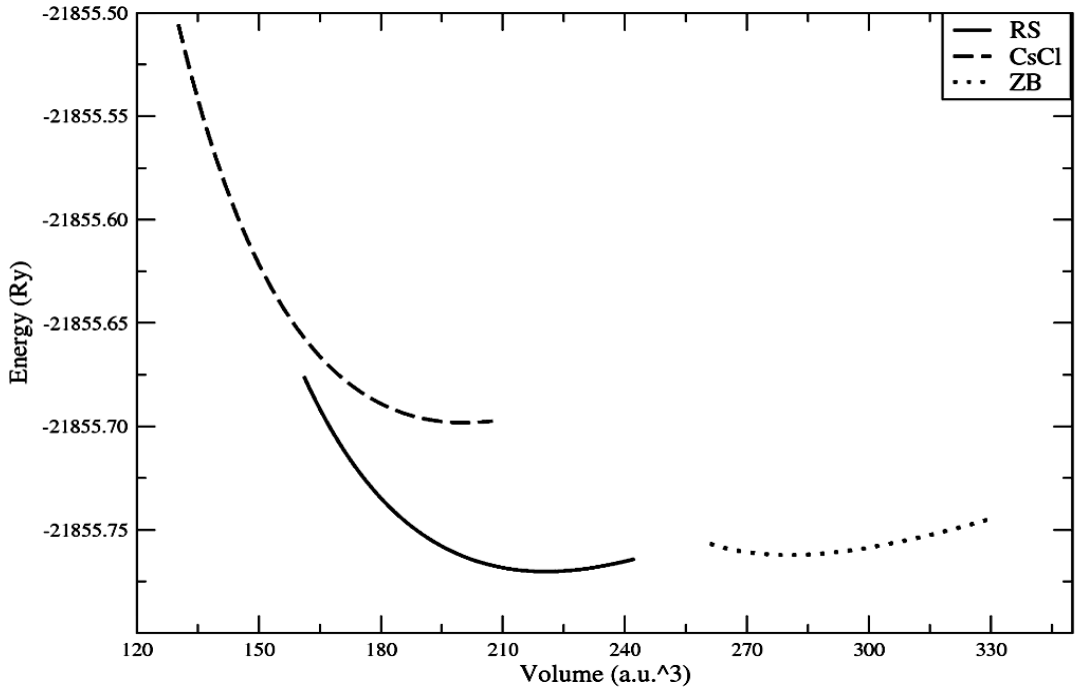

Figure 4.13: Total energy as function of volume of EuO compound in RS, CsCl and ZB phases using PBESOL-GGA method.

Figures 4.10 – 4.13 clearly show that the stable structures of EuO compound is rocksalt, it also shows that the transition may occur from RS to CsCl. The lattice parameters obtained from these figures are calculated due to the relation of the volume at minimum energy with the lattice parameter as mentioned before for the EuTe compound. The total energies are calculated using the equation of state fitted by Murnaghan's equation of state (Equation 3.9) [41].

Table 4.5 summarizes the results of the lattice parameters we obtained for EuO in the three structures using different methods of calculation. This Table also includes the available experimental and theoretical values.

Table 4.5: lattice constants a_o, bulk modulus B_o and pressure derivative of the bulk modulus B' of EuO in RS, CsCl and ZB structures using different methods of calculation.

Structures		**Present work**				**Other calculations**	**Experimental results**
		PBE-GGA	**LSDA**	**WC-GGA**	**PBEsol-GGA**		
RS	a_o **(Å)**	5.074	4.917	4.983	4.981	-	5.145[a], 5.14[b]
	B_o **(GPa)**	97.06	123.68	110.72	109.86	114[a], 118[a], 105[c]	110±5[b]
	B'	4.2	4.71	4.56	4.5	2.8[a], 2.2[a],3.2[c]	-
CsCl	a_o **(Å)**	3.097	2.996	3.039	3.037	-	-

	B_o (GPa)	107.63	132.7	120.81	118.98	-	-
	B'	3.9	4.44	4.21	4.23	-	-
ZB	a_o (Å)	5.496	5.353	5.408	5.406	-	-
	B_o (GPa)	95.36	99.50	87.20	85.91	-	-
	B'	8.85	5.59	5.59	5.03	-	-

[a] Ref. [12], [b] Ref. [11], [c] Ref. [14].

From Table 4.5, it is clearly seen that our results are in good agreement with experimental results with respect to RS structure. The lattice parameter obtained in this work using PBE-GGA method is less than that of the experimental value with 1.3% percentage error, and about 3% percentage error using PBEsol-GGA and WC-GGA. On the other hand, LSDA value, as always, is under estimated. B_o values are close to the available experimental [11, 12] and theoretical results [14]. The disagreement in the results of the first derivative bulk modulus in RS phase is due to the dependence of B' on many parameters such as temperature and pressure.

For CsCl and ZB structures, comparison is not available since results from experimental or other theoretical work are not available according to our knowledge. On the other hand, the comparison between RS and CsCl

lattice parameters shows that the lattice constant decreases as pressure increases. The bulk modulus also increases with increasing the pressure.

4.2.4 Structural phase transition of EuO compound:

In order to calculate the transition pressure, the curves of the total energy versus volume in RS, CsCl and ZB structures are needed. So the transition pressure can be evaluated using the slope of the common tangent, which is the derivative of the total energy with respect to the volume.

Figures 4.10 - 4.13 show the three phases (RS, CsCl and ZB) using different methods of calculation. These Figures show that the transition can occur between RS and CsCl phases. This indicates that the stable structure is RS, and the transition under high pressure can occur from RS to CsCl. This is consistent with the available experimental results [12].

The data we have got from these figures as well as the available experimental and theoretical results are arranged in Table 4.6.

Table 4.6: The transition pressure for EuO from RS to CsCl using different methods of calculation.

Method	Transition Pressure (P_t) in GPa		
	Present work	**Other calculations**	**Experimental results**
PBE-GGA	69.41	-	(47-63)[c], 40[d]
LSDA	61.17	48[a], 36[b]	
WC-GGA	64.16	-	
PBEsol-GGA	63.822	-	

[a] Ref. [14], [b] Ref. [15], [c] Ref. [12], [d] Ref. [11].

Our results indicate that the rocksalt phase is stable at low pressures, but this phase becomes unstable under high pressures, since the curves of RS and CsCl structures intersect, also CsCl curve is above the RS curve in the same range of unit cell volume. According to the experimental study done in 1995 by Heathman *et al* [12], they set up their experiment under high pressure up to 63 GPa. In their article, they mentioned that EuO undergoes pressure phase transition from RS to CsCl phase started at about 47 GPa, but the transition didn't end at 63 GPa [12]. This implies that our results are in excellent agreement with the experimental results, since the pressure we have got is the pressure at which transition ends (63 GPa) according to the experimental data.

4.3 Band Structure

4.3.1 Band structure of EuTe compound

The band gap energy (E_g)is defined as the energy that electrons must absorp to move from the valence band to the conduction band. So, the value of E_g determines whether the compound is metal, insulator or semiconductor. The band gap depends on temperature and pressure, but the relation between the band gap energy with pressure is only involved in this work. In order to calculate the band gap energy one need to define the Fermi enrgy (E_F) which is the highest energy level that electrons can occupy at absolute zero temperature.

The most features of the band gap energy for the three structures RS, CsCl and ZB of the EuTe compound are shown in Figures 4.14, 4.15, 4.16 and 4.17 using PBE-GGA, LSDA, WC-GGA and PBEsol-GGA methods, respectively.it is worth mentioning that LSDA method results are available in previous studies and it is repeated in order to make comparison easier with other new different methods.

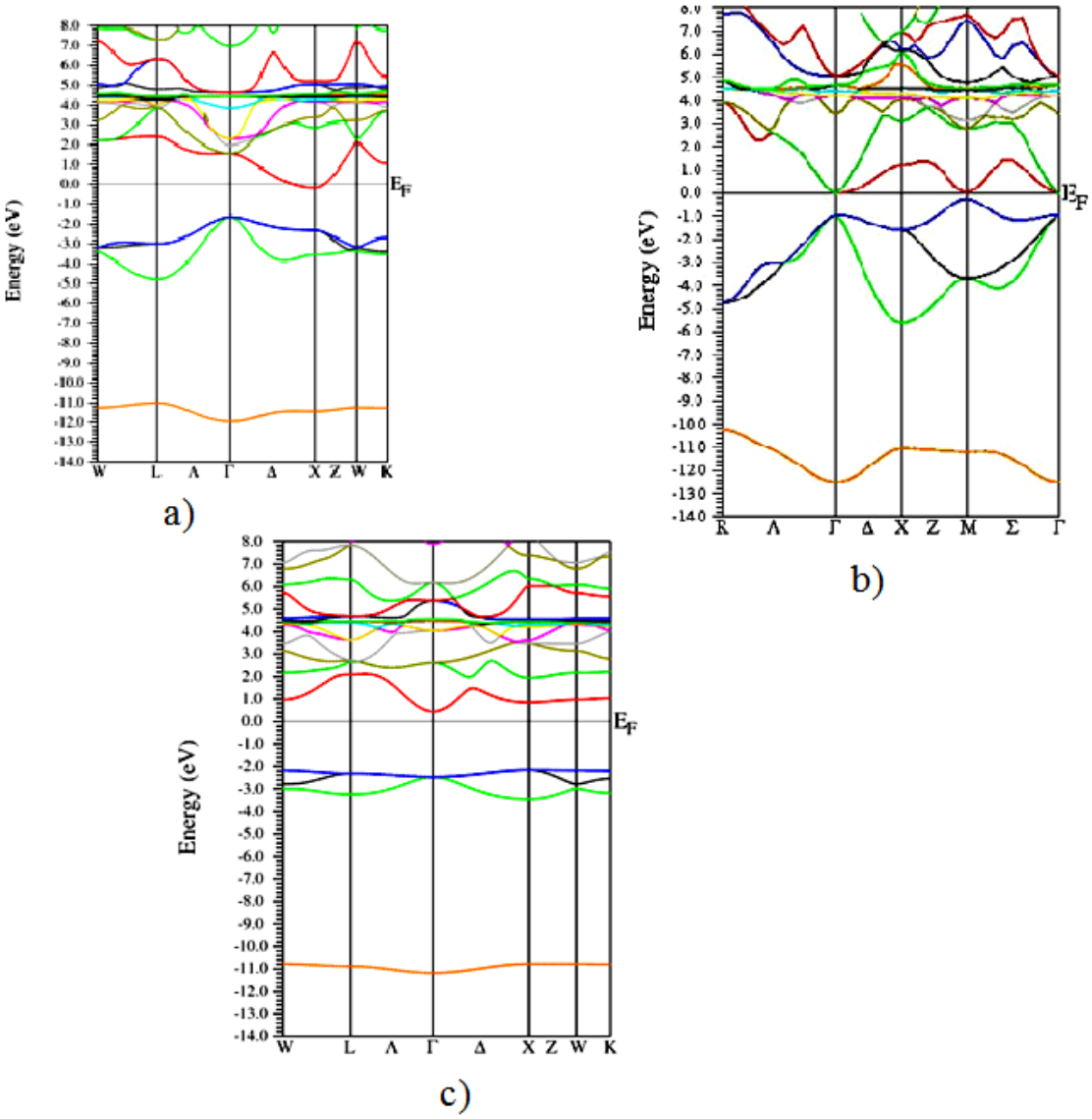

Figure 4.14: Band structure of a) RS, b) CsCl and c) ZB phases for EuTe along the principal high-symmetry directions in brillouin zone using PBE-GGA method.

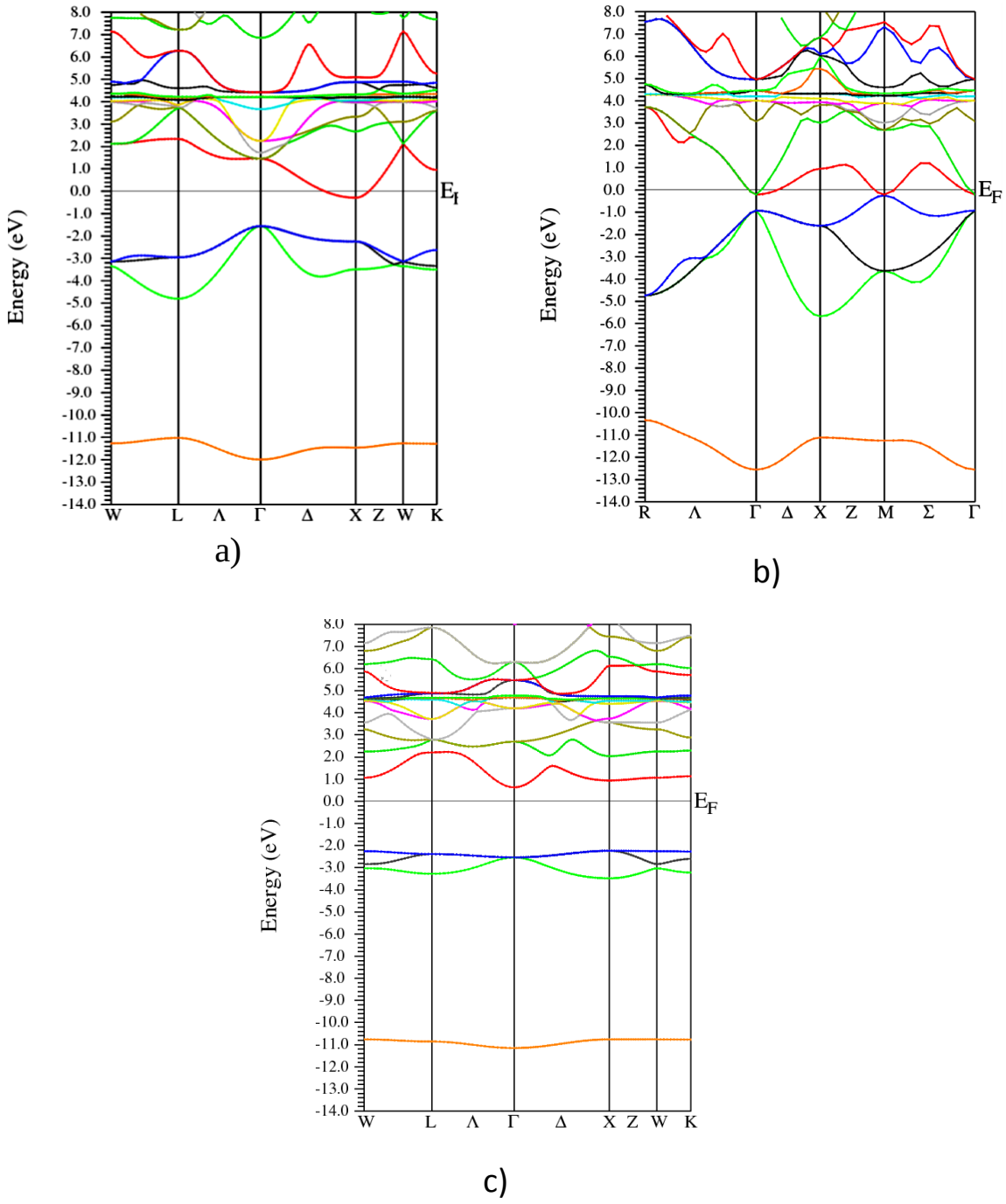

Figure 4.15: Band structure of a) RS, b) CsCl and c) ZB phases for EuTe along the principal high-symmetry directions in brillouin zone using LSDA method.

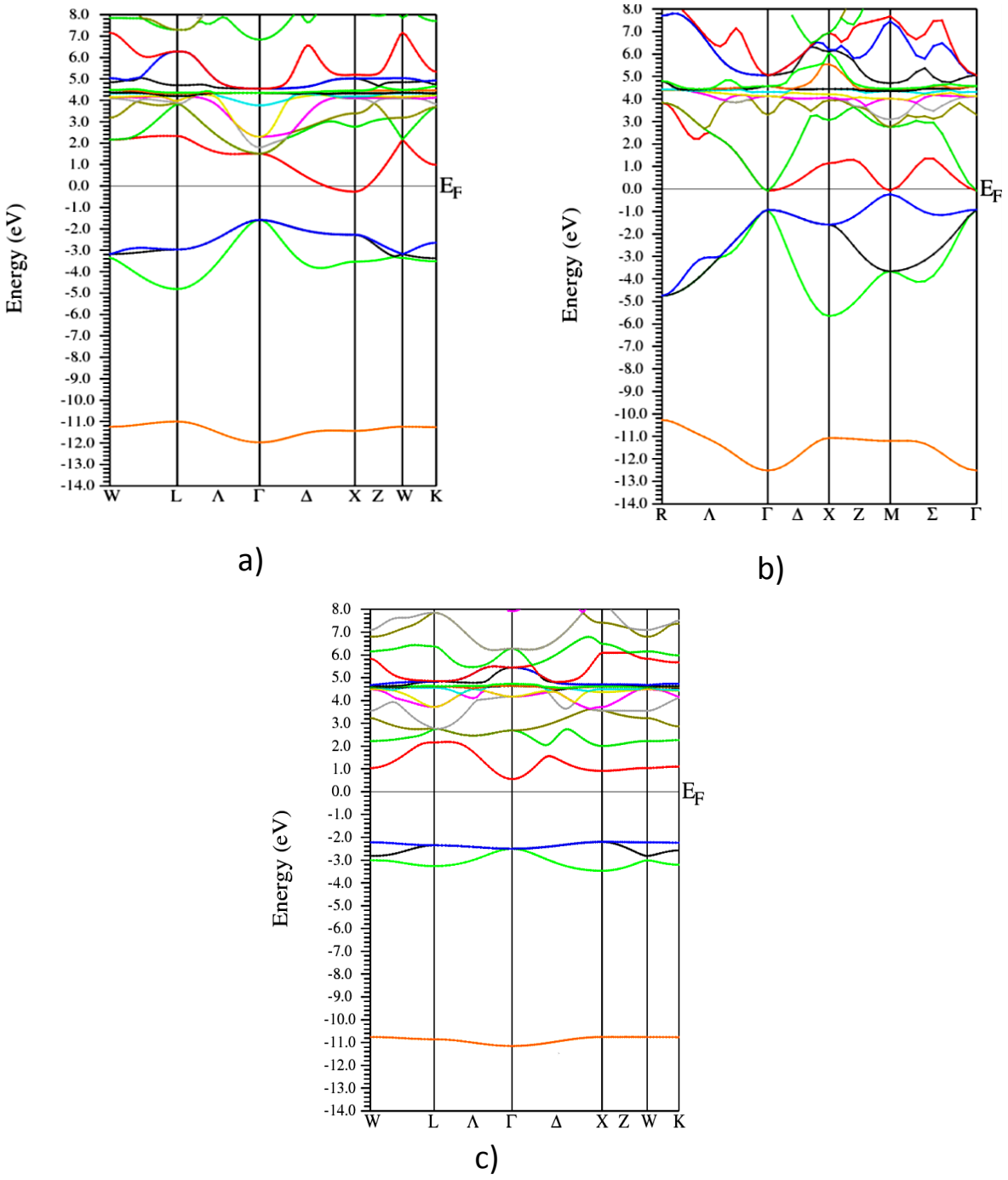

Figure 4.16: Band structure of a) RS, b) CsCl and c) ZB phases for EuTe along the principal high-symmetry directions in brillouin zone using WC-GGA method.

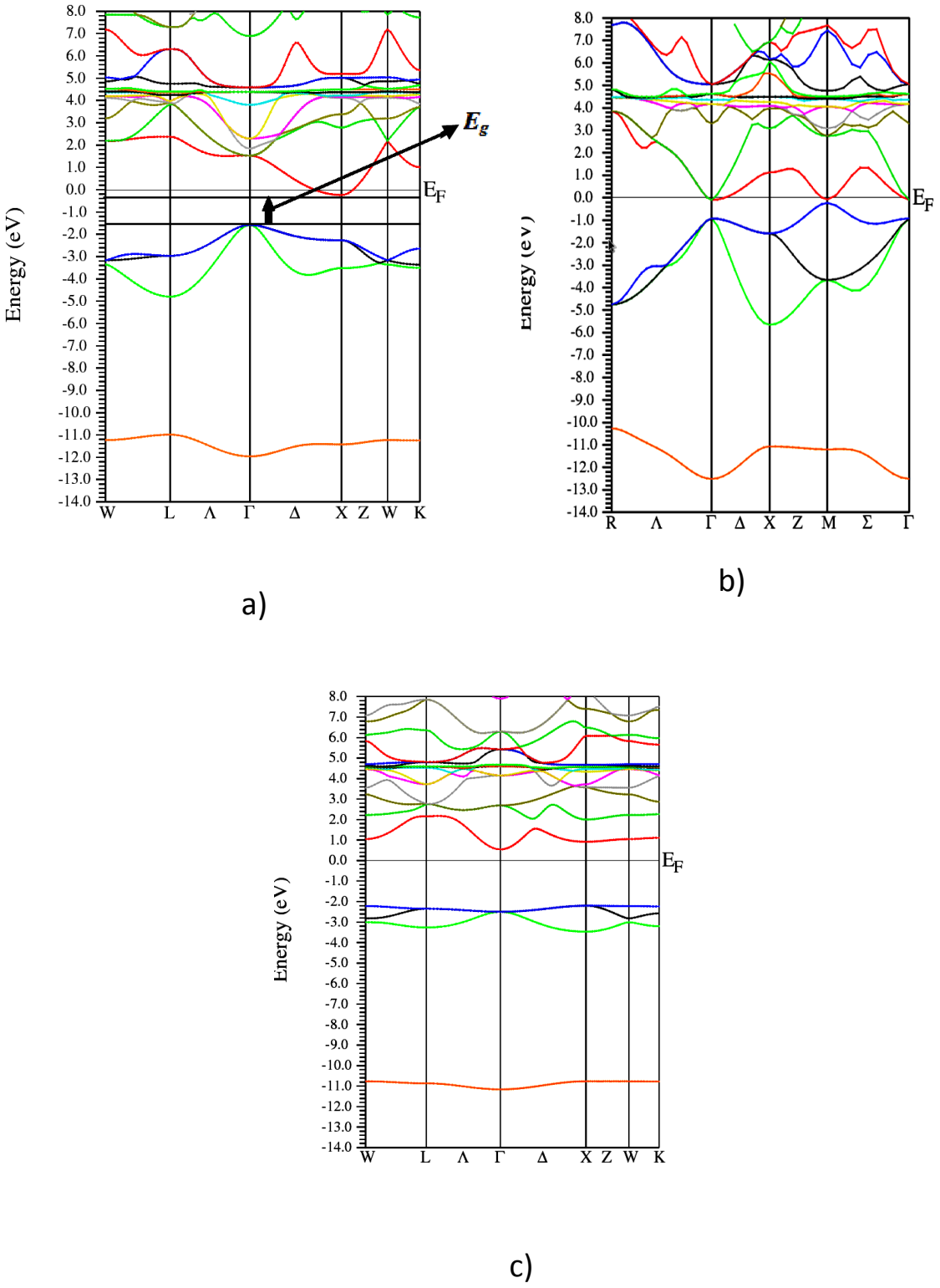

Figure 4.17: Band structure of a) RS, b) CsCl and c) ZB phases for EuTe along the principal high-symmetry directions in brillouin zone using PBEsol-GGA method.

The band gap energy appears from the difference between the top of the valence band (below the E_F energy level) and the bottom of the conduction band (upper the E_F energy level), (see Figure 4.17a), using the high symmetry lines (Γ, X, Δ, …..), which represents the x-axis, each line has specific position, for example (Γ line) has the position (0, 0, 0) $2\pi/ a_0$ as shown by figure 4.17a. Now, to determine whether this compound has direct or indirect band gap energy, take an example figure 4.17 a and b, if the band gap energy has the same high symmetry line such as (Γ- Γ) line, then we get direct band gap, on the other hand, if the high symmetry lines are different such as (Γ-X) lines as in Figure 4.17b, then it is named indirect band gap energy. The values of band gap energy for EuTe compound are summarized in Table 4.7.

Table 4.7: The band gap energy of EuTe in the RS, CsCl and ZB structures for spin down polarized electrons.

Structure	**Band gap energy E_g (eV)**				
	Present work				**Other calculations**
	PBE-GGA	**LSDA**	**WC-GGA**	**PBEsol-GGA**	
RS	1.43	1.26	1.32	1.34	1.1[a]
CsCl	0.92	0.71	0.84	0.82	
ZB	2.86	2.59	2.74	2.75	

[a] Ref. [16].

Table 4.7 indicates that the band gap energy ranges from (0.7 ~ 2.8) eV in the three structures. This implies that this compound is a semiconductor in

these structures, where the band gap energy of semiconductors ranges from 0.2 eV to less than 5 eV. Furthermore, Figures 4.13-4.16 show that RS and ZB structures have indirect band gap energy, while CsCl structure has direct band gap energy. It is worth noting that for all structures there is no experimental results are available according to our knowledge.

4.3.2 Band structure of EuO compound

Europium oxide (EuO) is one of the magnetic semiconductors. The important features of the band structure at high symmetry points for EuO compound in RS, CsCl and ZB structures are shown in Figures 4.18, 4.19, 4.20 and 4.21 using PBE-GGA, LSDA, WC-GGA and PBEsol-GGA methods, respectively. As it is seen in Figures 4.18, 4.19, 4.20 and 4.21, the band gap energy is indirect for RS and ZB structures, and it is direct for CsCl structure. The band gap energy of EuO is listed in Table 4.8 for different structures using different methods.

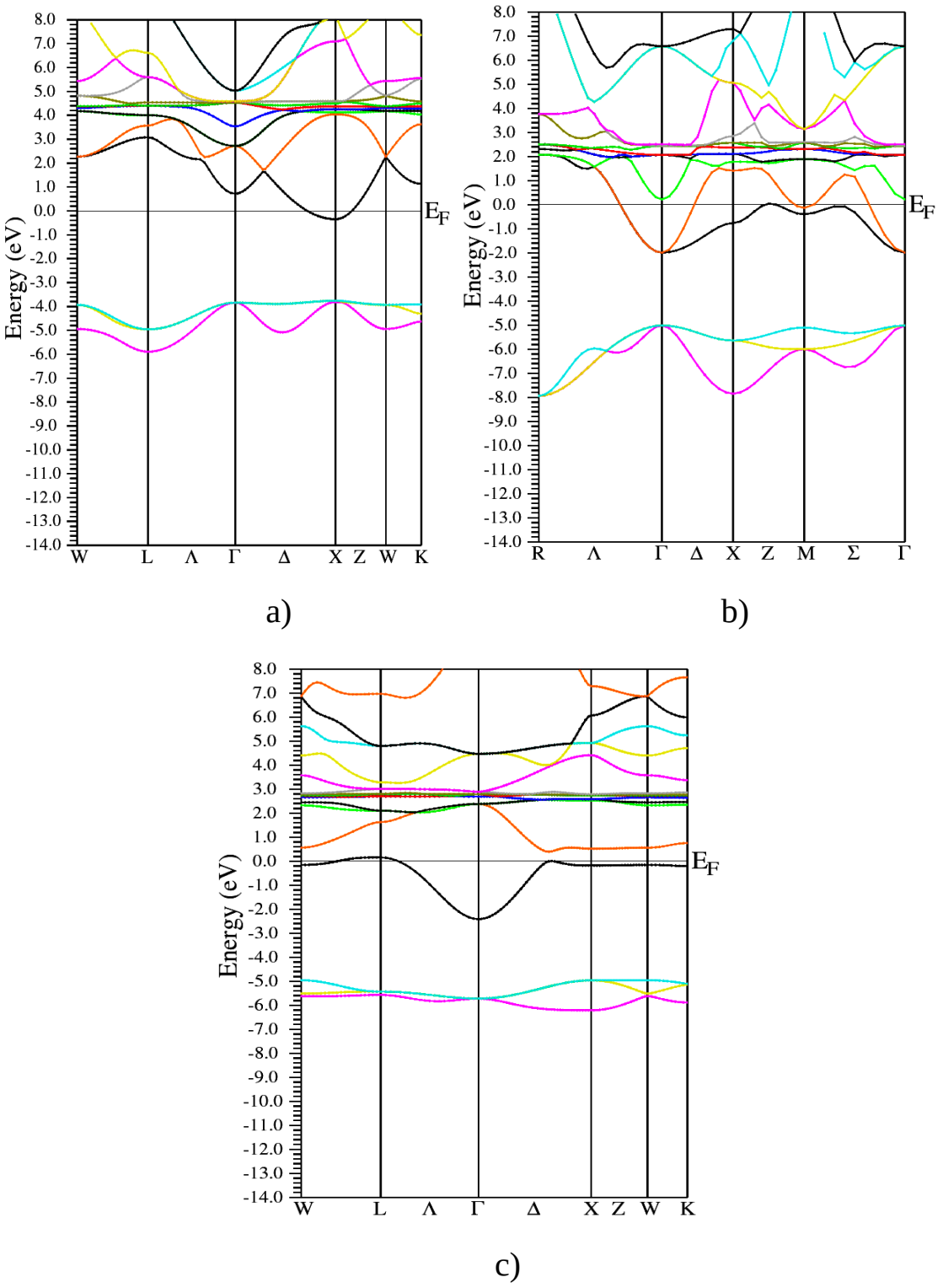

Figure 4.18: Band structure of a) RS, b) CsCl and c) ZB phases for EuO along the principal high symmetry directions in brillouin zone using PBE-GGA method.

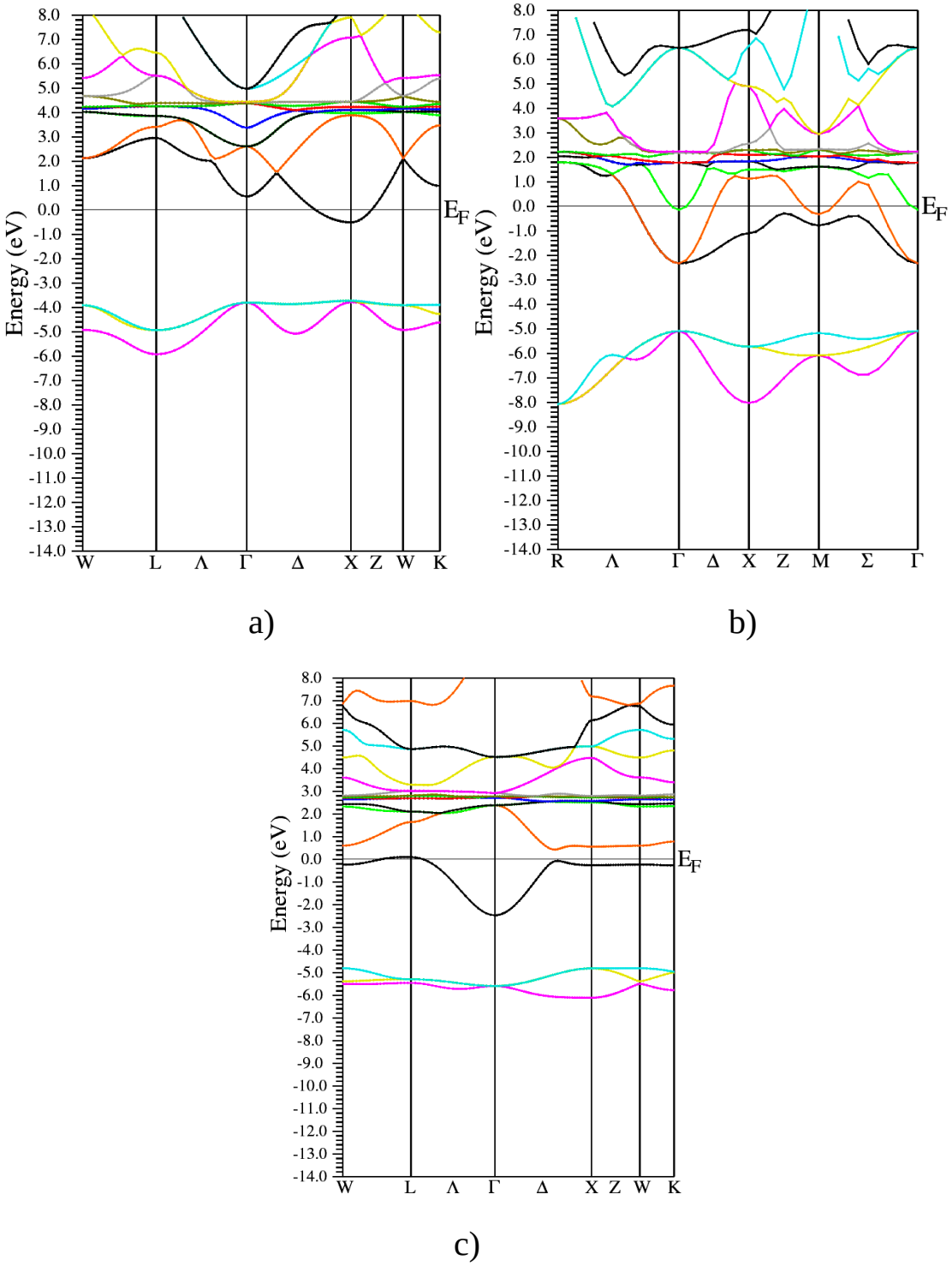

Figure 4.19: Band structure of a) RS, b) CsCl and c) ZB phases for EuO along the principal high-symmetry directions in brillouin zone using LSDA method.

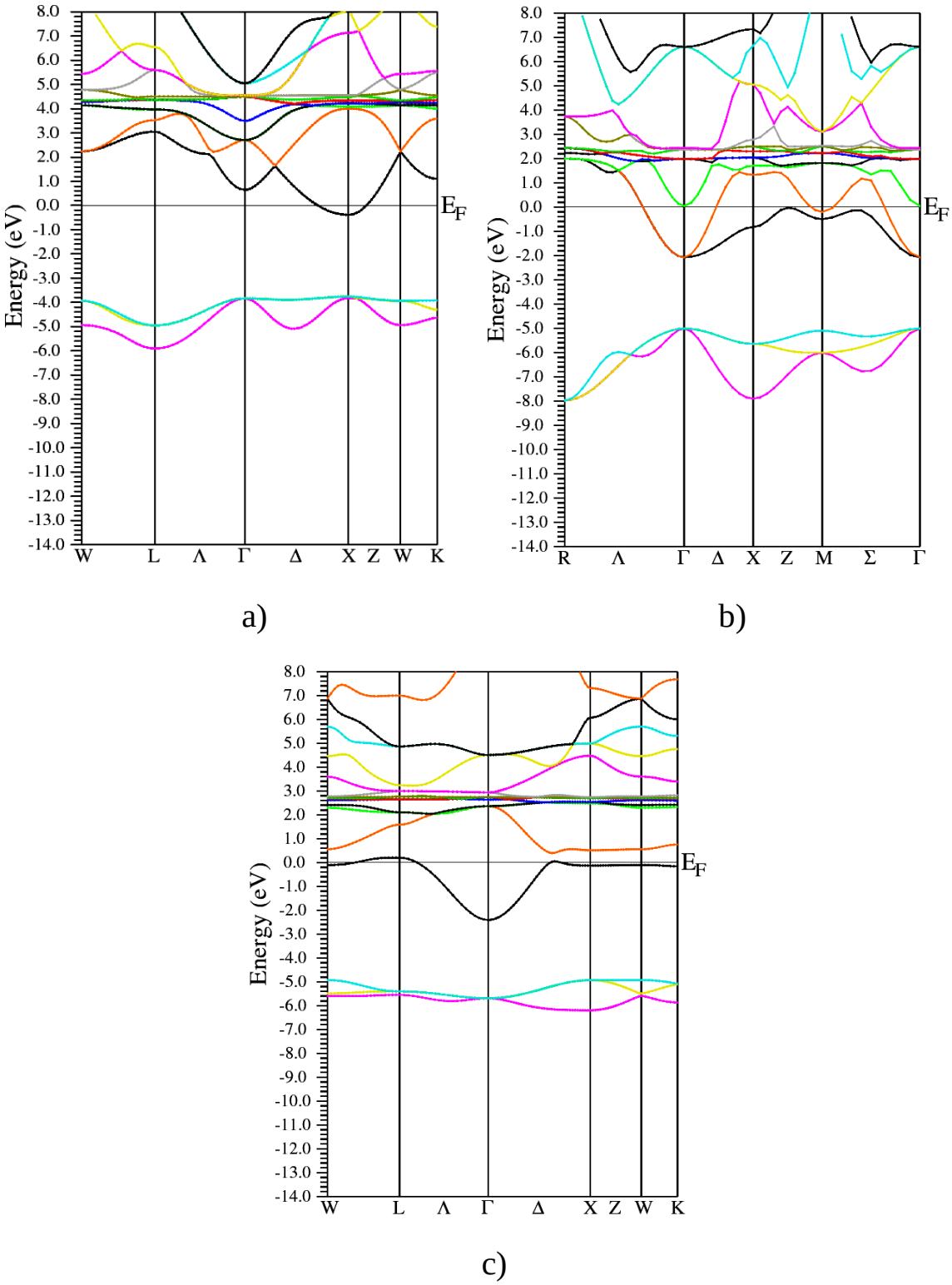

Figure 4.20: Band structure of a) RS, b) CsCl and c) ZB phases for EuO along the principal high- symmetry directions in brillouin zone using WC-GGA method.

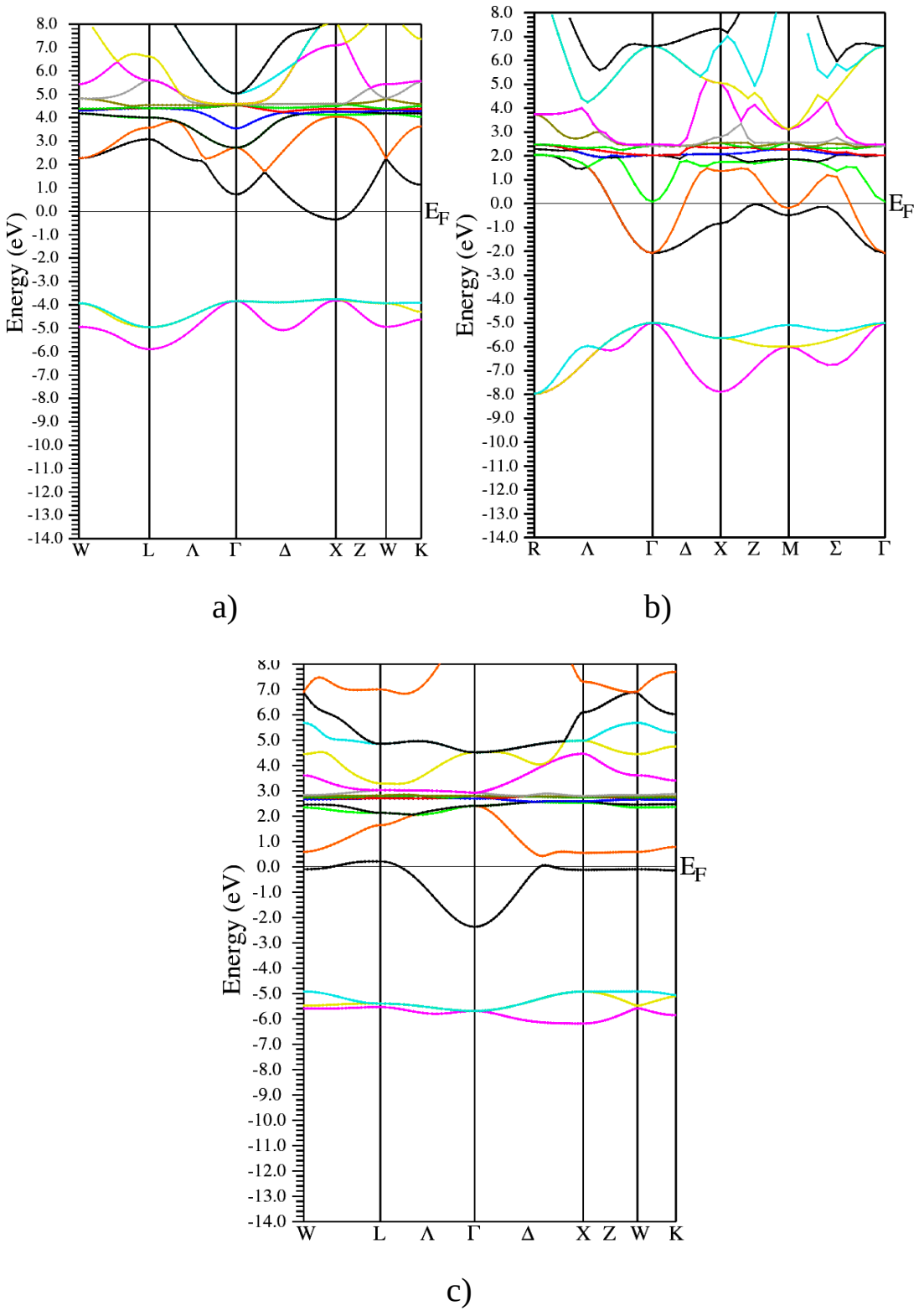

Figure 4.21: Band structure of a) RS, b) CsCl and c) ZB phases for EuO along the principal high-symmetry directions in brillouin zone using PBESOL-GGA method.

The band gap energy of EuO compound is calculated in RS, CsCl and ZB structure using different methods of calculations, using the same procedure used in EuTe compound before. Table 4.8 summarizes these values of E_g

Table 4.8: The band gap energy of EuO in the RS, CsCl and ZB structures for spin down polarized electrons.

Structure	**Band gap energy E_g (eV)**				
	Present work				**Other calculations**
	PBE-GGA	**LSDA**	**WC-GGA**	**PBEsol-GGA**	
RS	3.58	3.29	3.44	3.41	3.4[a]
CsCl	3.02	2.76	2.93	2.92	
ZB	2.55	2.34	2.52	2.55	

[a] Ref. [16] using SIC-LSDA.

The results shown in table 4.8 confirm that EuO is a semiconductor, since it has band gap energy at the range of (0.2-5) eV, also these results consistent with other calculated results [16]. The data presented in Table 4.8, indicate that the band gap energy decreases as the structure undergoes from RS to ZB. This implies that the energy gap between valence and conduction levels decreases with increasing pressure.

It is worth to mention that our results agree well with other calculations for RS structures especially for the results of E_g obtained using PBEsol-GGA and WC-GGA. Comparison cannot be completed for other structures because there are no experimental and other theoretical results available according to our knowledge.

Chapter 5

Conclusion

In this work we have used the Full-potential augmented plane wave (FP-LAPW) approach within the density functional theory (DFT) in the local – spin-density approximation (LDA/ LSDA) and the generalized gradient approximation (GGA) for the exchange correlations functional as implemented by WIEN2K to calculate the ground-state energies, lattice parameters, bulk modulus and their derivatives, transition pressures and energy band gap.

In this study we have obtained the following results:

1- The magnetic and electronic properties are found to be in good agreement with the available experimental results.
2- The stable magnetic state for both compounds has been studied under the ambient pressure and at absolute zero temperature (T=0).
3- The stable structure of EuTe and EuO compounds has been found to be rocksalt structure, and the transition from rocksalt to cesium chloride structure is found to take place at about 11GPa for EuTe, and completed transition for EuO has taken place at about 64 GPa.

Table 5.1 summarizes the results of the band gap energy of EuTe and EuO compounds using different methods of calculation.

Table 5.1: The results of the band gap energy of both EuTe and EuO compounds using different methods of calculation.

Structure	Band gap energy E_g (eV)							
	EuTe				EuO			
	PBE-GGA	LSDA	WC-GGA	PBEsol-GGA	PBE-GGA	LSDA	WC-GGA	PBEsol-GGA
RS	1.43	1.26	1.32	1.34	3.58	3.29	3.44	3.41
CsCl	0.92	0.71	0.84	0.82	3.02	2.76	2.93	2.92
ZB	2.86	2.59	2.74	2.75	2.55	2.34	2.52	2.55

This study shows that both compounds are magnetic semiconductors in the three structures (RS, CsCl and ZB structures) with wide band gap energy except for EuTe compound in CsCl structure.

Since PBE-GGA, LSDA, WC-GGA and PBEsol-GGA methods are used in this study, comparison between these methods shows that PBEsol-GGA and WC-GGA are recommended methods in calculating the transition pressure, bulk properties and band gap energy, while PBE-GGA is recommended in calculating the lattice constant.

REFERENCES

[1] Nobel prizes committee. (nobelprize.org/nobel_prizes/physics), Sweden; 2000, 2007. Available from: www.nobelprize.org/nobel_prizes/physics

[2] Kunes, J. Ku W. and Pickett, W. E. **"Exchange Coupling in Eu Monochalcogenides from First Principles"**. J. Phys. Soc. Jpn. 2005; 74 (5): 1408-1411.

[3] Holleman, A. F. and Wiberg, E."**Inorganic Chemistry".** San Diego Academic Press; 2001.

[4] Cooley, R. A. Yost, D. M. and Stone, H.W. "**Europium (II) Salts. Inorganic Syntheses. Inorganic Syntheses.2 ".** 1946; 69–73.

[5] Hamric, D. **"Rare-Earth Metal Long Term Air Exposure Test"**. Metallium Inc. 2009-8-8.

[6] Shapira, Y. Foner, S. and Reed, T. B. "**EuO. I. Resistivity and Hall Effect in Fields up to 150 kOe".** Phys. Rev. B8. 1973; 2299-2315.

[7] Kaminski, B. Lafrentz, M. Pisarev, R. V. Yakovlev, D. R. Pavlov, V. V. Lukoshkin, V. A. Henriques, A. B. Springholz, G. Bauer, G. Abramof, E. Rappl, P. H. O. and Bayer, M. **"Optical Second Harmonic Generation in the Centrosymmetric Magnetic Semiconductors EuTe and EuSe"**. Phys. Rev. B 81. 2010; 155201-1-8.

[8] Akimoto, R. Kobayashi, M. and Suzuki, T. "**High-Pressure Study of Photoluminescence Spectra in Magnetic Semiconductor EuSe"**. J. Phys. Soc. Jpn. 1993; 62. 1490-1493.

[9] Rooymans, C. J. M. **"High Pressure Phase Transition of Europium Telluride"**. Solid State Commun. 1965; 3: 421.

[10] Chatterjee, A. Singh, A. K. and Jayaraman, A. **"Pressure-Induced Electronic Collapse and Structural Changes in Rare-Earth Monochalcogenides"**. Phys. Rev. B 6. 1972; (6): 2285–2291

[11] Jayaraman, A. Singh, A. K. Chatterjee, A. and Usha Devi, S. **"Pressure-Volume Relationship and Pressure-Induced Electronic and Structural Transformations in Eu and Yb Monochalcogenides".** Phys. Rev. B 9. 1974; (6): 2513–2520.

[12] Heathman, S. Le Bihan, T. Darracq, S. Abraham, C. De Ridder, D. J. A. Benedict, U. Mattenberger, K. and Vogt, O. **"High Pressure Behaviour of TmTe and EuO".** J. Alloys Comp. 1995; 230: 89-93.

[13] Moodera, J. S. Santos, T. S. and Nagahama. T. **"The Phenomena of Spin-Filter Tunneling"**. J. Phys.: Condens. Matter. 2007; 19: 165202-1-5.

[14] Wan, X. Dong, J. and Savrasov, S. Y. "**Electronic Structure Calculation of Magnetic Exchange Interactions in Europium Monochalcogenides"**. Cond. Mat. Matrl-Sci. 2010; 1-5.

[15] Gour, A. Singh, S. Singh, R. K. and Singh, M. Pramana- J. Phys. "**Pressure-Induced Phase Transition and Stability of EuO and EuS with NaCl Structure"**. 2008; 71 (1): 181-186.

[16] Horne, M. Strange, P. Temmerman, W. M. Szotek, Z. Svane, A. and Winter, H. "**The Electronic Structure of Europium Chalcogenides and Pnictides"** J. Phys.: Condens. Matter 2004; 16: 5061-5070.

[17] Goncharenko, N. and Mirebeau, I. "**Magnetic Order in EuTe under Pressure up to 17 GPa: A neutron Study"**. Eyrophys. Lett. 1997; 37 (9): 633-638.

[18] Singh, D. Srivastava, V. Rajagopalan, M. Husain, M. and Bandyopadhyay, A. K. "**High-Pressure Band Structure and Structural Stability of EuTe".** Phys. Rev. B 64. 2001; 115110-1-6.

[19] Cottenier, S. **Density Functional Theory and the Family of (L)APW-Methods: A step-by-step Introduction. Belgium: Instituut voor Kern-en Stralingsfysica**, K.U. Leuven; 2002.

[20] Hohenberg P. and Kohn W. "**Inhomogeneous Electron Gas".** Phys. Rev. 1964; 136 (3B): B 864-B 871.

[21] Schiff, L.I. **Quantum Mechanics**. New York: McGraw-Hill; 1986.

[22] Kohn W. and Sham, L. "**Self Consistent Equations Including Exchange and Correlation Effects"**. Phys. Rev. 1965; 140 (4A): A1133-A1138.

[23] Parr, R. G. Yang, W. **Density-Functional Theory of Atoms and Molecules**. Oxford: Oxford University Press; 1994.

[24] Payne, M. C. Teter, M. P. Allan, D. C. Arias T. A. and Joannopoulos J. D. **"Itrative Minimization Techniques for ab-initio Total-Energy Calculations: Molecular Dynamics and Conjugate Gradients".** Revs. Mod. Phys. 1992; 64 (4): 1045-1055.

[25] Szabo A. and Ostalund N. S. **Modern Quantum Chemistry**. New York: McGraw-Hill, Inc.; 1989. p53.

[26] Vosko, S. H. Wilk, L. and Nusiar, M. **"Accurate Spin-Dependent Electron Liquid Correlation Energies for Local Spin Density Calculations: A Critical Analysis"**. Can. J. Phys.1980; 58 (8): 80-159.

[27] Wigner, E. **"On the interaction of electrons in metals".** Phys. Rev. 1934; 46: 1002-1011.

[28] Perdew, J. P. and Zunger, A. **"Self-Interaction Correction to Density-Functional Approximations for Many-Electron Systems".** Phys. Rev. B 23. 1981; 5048-5079.

[29] Ceperley D. M. and Alder, B. J. **"Ground State of the Electron Gas by A stochastic Method".** Phys. Rev. Lett. 1980; 45: 566-569.

[30] Perdew, J.P. **"Accurate Density Functional for the Energy: Real-Space Cutoff of the Gradient Expansion for the Exchange Hole".** Phys. Rev. Lett. 1985; 55 (16): 1665-1668.

[31] Slater, J. C. **The Self-Consistent Field for Molecules and Solids, Quantum Theory of Molecules and Solid**. Vol. 4. New York: McGraw-Hill; 1974.

[32] Slater, J. C **"Wave Functions in a Periodic Potential".** Phys. Rev. 1937; 51 (10): 846-851.

[33] Andersen, O. K. "**Linear Methods in Band Theory**". Phys. Rev. B 12. 1975; 3060.

[34] Sjostedt, E. Augmented Planewaves**, Developments and Applications to Magnetism**. Sweden: Acta Universitatis Upsaliensi; 2002.

[35] Plaha, P. Schwarz, K. Madsen, G. Kvasnicka D. and Luitz, J. Wien2k, **An augumented Plane Wave + Local Orbitals Program for Calculating Crystal Properties**. Karlheinz Schwarz Techn. Austria: Universitat Wien; 2001.

[36] Singh, D. "**Ground-State Properties of Lanthanum: Treatment of Extended-Core States"**. Phys. Rev. B 43. 1991; 6388.

[37] Madsen, G. K. H. Blaha, P. Schwarz, K. Sjostedt, E. Nordstrom, L. **"Efficient Linearization of the Augmented Plane-Wave Method"**. Phys. Rev. B 64. 2001; 195134-1-9.

[38] Perdew, J. P. Ruzinszky, A. Csonka, G. I. Vydrv, O.A. Scuseria, G.E. Constantin, L. A. Zhou, X. and Burke, K. "**Restoring the Density-Gradient Expansion for Exchange in Solids and Surfaces"**. Phys. Rev. Lett. 2008; 100 (13): 136406-1-4.

[39] Perdew, J.P. and Wang, Y. **"Accurate and Simple Analytic Representation of the Electron-Gas Correlation Energy".** Phys. Rev. B 45. 1992; (23): 13244-13249.

[40] Monkhorst, H. J. and Pack, J .D. " **Special Points for Brillouin-Zone Integrations".** Phys. Rev. B 13. 1976; 5188–5192.

[41] Murnaghan, F. D. **"The Compressibility of Media under Extreme Pressures**". USA: Proc. N. A. Sc.; 1944. 30: pp. 244–247.

جامعة النجاح الوطنية
كلية الدراسات العليا

الضغط المرتفع والاستقرار التركيبي للمركبات EuTe وEuO

إعداد

رويدة فخري محمد دويكات

إشراف

د. محمد سلامة أبو جعفر
د. عبد الرحمن أبو لبدة

قدمت هذه الأطروحة استكمالاً لمتطلبات الحصول على درجة الماجستير في الفيزياء بكلية الدراسات العليا في جامعة النجاح الوطنية نابلس، فلسطين.

2012م

الضغط المرتفع والاستقرار التركيبي للمركبات EuTe و EuO

إعداد

رويدة فخري محمد دويكات

إشراف

د. محمد سلامة أبو جعفر

د. عبد الرحمن أبو لبدة

الملخص

لقد تم حساب الخصائص الإلكترونية والمغناطيسية للمركبات شبه الموصلةEuTe و EuO في حالة التراكيب البلورية التالية الملح الحجري وكلوريد السيزيوم والزنك بلند، باستخدام طريقة الموجات المستوية المعدلة الخطية للجهد تام (FP-LAPW) من خلال تقريب الكثافة المغزلية الموضعية (LSDA)وتقريب الميل الاتجاهي المعمم (GGA) للجهد التبادلي الترابطي. واستخدم برنامج (WIEN2K-code) في حساباتنا.

لقد تم دراسة تأثير الضغط المرتفع على الخصائص الإلكترونية للمركبين EuTe و EuO وقد أظهر كلا المركبين أن تركيب الملح الحجري هو التركيب المستقر. لكن تحت تأثير الضغط المرتفع ينتقل كلا المركبين من تركيب الملح الحجري إلى التركيب كلوريد السيزيوم وذلك عند الضغط 12 جيجا باسكال و8 جيجا باسكال و10 جيجا باسكال و 11 جيجا باسكال للمركب EuTe باستخدام الطرق التالية بالتتالي PBE-GGA و LSDA وWC-GGA و GGA، والإنتقال لتركيب كلوريد السيزيوم اكتمل للمركب EuO تقريبا عند 69 جيجا باسكال و 61 جيجا باسكال و 64 جيجا باسكال و 63 جيجا باسكال باستخدام الطرق التالية بالتتالي PBE-GGA و LSDA وWC-GGA و PBEsol-GGA.

وقد وجد أيضا أن المركبات أشباه موصلات تحت الظروف العادية وتحت الضغط المرتفع في تراكيبها الثلاثة التي درست في هذا البحث. وأظهرت حسابات التركيب الحزمي أن مركب EuTe يحتوي على فجوة طاقة غير مباشرة في كل من تركيب RS وZB، لكنها كانت صغيرة ومباشرة في

تركيب CsCl. أيضاً فجوة الطاقة لمركب EuO كانت غير مباشرة في التراكيب RS و ZB ولكنها مباشرة في تركيب CsCl.

إضافةً إلى ذلك، فإن المقارنة بين الطرق المختلفة للحسابات أظهرت أن طريقة PBE–GGA كانت أفضل في التنبؤ لقيمة ثابت الشبكة في تركيب RS، لكن طريقتي WC–GGA و PBEsol–GGA كانتا أفضل في التنبؤ لقيمة كل من معامل الصلابة (B_0) وضغوط التحول للمادة (P_t).